Bachelor Thesis FS2021

Lucerne University of Applied Sciences and Arts

Simulation and Measurement of Scattered Radiation in X-Ray Computed Tomography

Student:	Riccardo Dario Dirnberger
Supervisor:	Prof. Dr. Philipp Schuetz
Expert:	Dr. Iwan Jerjen
Industry Partner:	Dr. Jorge Martinez Garcia

Lucerne, 11 June 2021

Bachelor-Thesis an der Hochschule Luzern - Technik & Architektur

Titel	**Simulation and Measurement of Scattered Radiation in X-Ray Computed Tomography**
Diplomandin/Diplomand	**Dirnberger, Riccardo Dario**
Bachelor-Studiengang	**Bachelor Medizintechnik**
Semester	**FS21**
Dozentin/Dozent	**Schuetz, Philipp**
Expertin/Experte	**Jerjen, Iwan**

Abstract Deutsch
Seit dem Sommer 2020 hat die Hochschule Luzern für Technik und Architektur (HSLU T&A) ein CT-System namens LuCi (Lucerne Ct Imaging) für Forschungszwecke zur Verfügung. Die Streustrahlung innerhalb eines solchen Systems ist einer der Hauptstörfaktoren, welcher die Genauigkeit der Rekonstruktion eines gemessenen Objekts beeinträchtigt. Daher werden eine Analyse und Quantifizierung des Streustrahlungsbeitrags in LuCi benötigt, welche das Ziel dieser Bachelor-Thesis sind. Eine Literaturrecherche hat ergeben, dass die Monte Carlo Methode ein zuverlässiges Werkzeug für die Simulation von Streustrahlung ist. Ein Simulationswerkzeug, welches diese Methode implementiert ist GATE, eine Open-Source Software basierend auf GEANT4, einem Toolkit, das für die Simulation des Durchgangs von Teilchen durch Materie benutzt wird. Ein Simulationsaufbau eines virtuellen Nachbaus von LuCi wurde entwickelt und der Streustrahlungsbeitrag für verschiedene Konfigurationen simuliert. Die verwendete Röntgenquelle war ein Kegelstrahl mit einem Quellenspektrum für eine Beschleunigungsspannung von 160 kV und einem 6.5 µm dickem Wolframtarget. Aus den Simulationsergebnissen der Konfigurationen wurde der Streustrahlungsbeitrag der Einzelteile berechnet. Der grösste Beitrag von 1.89% wurde für die Granitblöcke berechnet, beim Gehäuse liegt der Beitrag bei 0.60% und der kleinste Streustrahlungsbeitrag von 0.56% wurde für die Detektor- und Objekthalterung berechnet. Für den gesamten Simulationsaufbau, bestehend aus Phantom, Gehäuse, Granitblöcken, Detektor- und Objekthalterung, wurde eine Streustrahlung von 6.25±0.40% berechnet. Zur gleichen Zeit wurden experimentelle Messungen der Streustrahlung an LuCi an der HSLU vom Team von CC TES (Competence Centre Thermische Energiespeicher) durchgeführt, welche ein Ergebnis von 12.57±0.34% ergaben. Verglichen mit den Simulationsergebnissen ergibt sich ein Unterschied von 6.32%. Aufgrund des grossen Unterschieds zwischen experimentell erhobenen und simulierten Ergebnissen sind weitere Untersuchungen des Simulationsaufbaus erforderlich.

Abstract Englisch
Since summer 2020, a CT system called LuCi (LUcerne Ct Imaging) is available for research purposes at Lucerne University of Applied Sciences and Arts (LUASA). Scattered radiation within such a system is an important deteriorating factor impacting the accuracy of reconstruction of a measured object. Therefore, the analysis and quantification of scattered radiation contribution in LuCi is required, which is the aim of this bachelor thesis. Research has shown that the Monte Carlo method is a reliable tool for the simulation of scattered radiation. A simulation tool implementing this method is GATE, an open-source software based on GEANT4, which is a toolkit used for the simulation of the passage of particles through matter. A simulation setup representing LuCi virtually was developed, and the scattered radiation simulated for different configurations. The implemented source was a cone beam with a source spectrum for a 160 kV acceleration voltage and a 6.5 µm thick tungsten target. From the simulation results of the configurations, the scattered radiation contribution of individual parts was calculated. The biggest contributors are the granite blocks, with a contribution of 1.89%; a value of 0.60% was calculated for the cabinet, and the smallest contributor to the scattered radiation, at 0.56%, are the detector holder and object holder. For the full simulation setup, including phantom, cabinet, granite blocks, detector holder and object holder, a scattered radiation of 6.25±0.40% was calculated. Simultaneously, experimental measurements of the scattered radiation within LuCi were carried out at LUASA by the Competence Centre Thermal Energy Storage (CC TES) team, showing a result of 12.57±0.34%, resulting in a difference of 6.32% in comparison to the simulation results. Given the large difference between the experimentally measured and simulated results, further research into the simulation setup is needed.

Ort, Datum Luzern, 11.06.2021

List of Abbreviations

cab	cabinet
cabs	cabinet “sandwich”
CC TES	Competence Centre Thermal Energy Storage
CT	Computed Tomography
dh	detector holder
GATE	Geant4 Application for Tomographic Emission
GEANT4	GEometry ANd Tracking 4
gran	granite
LUASA	Lucerne University of Applied Sciences and Arts
LuCi	LUcerne Ct Imaging
ODD	Object Detector Distance
oh	object holder
PET	Positron Emission Tomography
p	phantom
pmx-	phantom moved in direction x-
SD	Standard Deviation
SDD	Source Detector Distance
SPECT	Single Photon Emission Computed Tomography
SPR	Scatter-to-Primary-Ratio
vGATE	Virtual Geant4 Application for Tomographic Emission

Table of Contents

1 Introduction

The subject of this bachelor thesis is the simulation and measurement of scattered radiation in X-ray computed tomography (CT).

1.1 Background

CT is an imaging technology increasingly used in the industry for inspection, evaluation and analysis, owing to the fact that it offers a non-destructive testing technique (Copley et al., 1994).Since summer 2020, a CT system called LuCi (LUcerne Ct Imaging) has been available for research purposes at Lucerne University of Applied Sciences and Arts (LUASA). The possible applications are numerous. One current area of frequent application at LUASA is the evaluation of thermal energy storage solutions (Hochschule Luzern, 2020).

An important deteriorating factor regarding the accuracy of reconstruction of a measured object is scattered radiation. This form of radiation is called secondary radiation and is comprised of photons which undergo scattering effects when they come into contact with the phantom or its environment. The resulting effects in CT images are artefacts. Hence, the reduction of scattered radiation is essential for high-quality CT images. To achieve this objective, the form and amount of scattered radiation must be analysed and quantified. There are two main strategies: firstly, scattered radiation can be estimated experimentally by taking specific measurements while using phantoms; secondly, simulation programmes can be used to estimate its effects.

1.2 Scattered radiation

Scattered radiation is a form of secondary radiation and is caused by the interaction of an X-ray beam and an object. During a CT scan, the X-ray beam irradiating an object is attenuated. The intensity of the X-ray photons travelling through matter decreases (almost) exponentially. This process of exponential attenuation is described by the Beer-Lambert law for a monochromatic narrow X-ray beam. The attenuation is caused by the interaction of some of the photons with the atoms within the irradiated material. As illustrated in Figure 1, there are two types of photons. Primary photons do not interact with the material, whereas secondary photons are either absorbed or scattered. The scattered radiation (secondary photons) is caused by different physical effects (Schoerner, 2012).

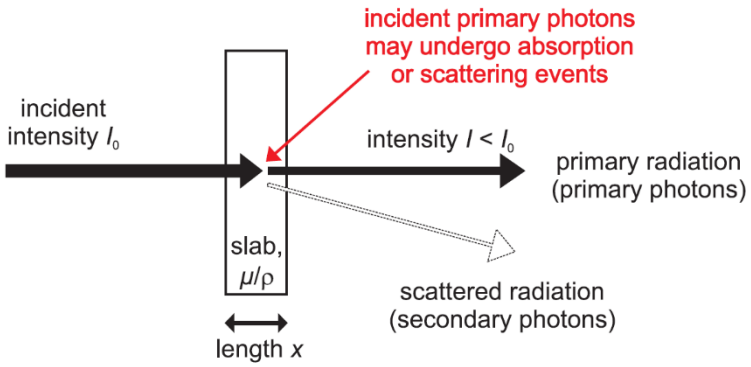

Figure 1: Schematic illustration of the interaction of an X-ray beam with an object, the attenuation and the absorption or scattering of the photons caused (Schoerner, 2012)

The total amount of scattered radiation can be split into two groups: scattered radiation caused by the object/phantom; and environmental scattering, which is caused by the CT scanner's surroundings, that is, the cabinet, detector, detector holder and object/phantom holder. The magnitude of its effect depends on the material, the size of the phantom and the distance between phantom and detector. More detail regarding the influence of the material is given in section 1.2.1.
In general, it can be observed that the scatter-to-primary ratio (SPR) increases with bigger phantoms and when the distance between sample and detector is increased (Kalender, 1981). The SPR is defined as the scattered radiation energy divided by the energy of the primary beam striking the same area on the detector. The environmental scattering is influenced by the system's cabinet as well as the mechanical parts placed within it. These mechanical parts are often essential to the system setup, which is why complete elimination of environmental scattering is difficult (Schoerner, 2012).

1.2.1 Physical effects

The main scattering effects caused by the interaction of photons with atoms are the photoelectric effect, Rayleigh/Thomson (coherent) scattering and Compton (incoherent) scattering. During the photoelectric effect, the incident photon interacts with a bound electron of the absorber atom, resulting in the absorption of the photon and the excitation or ejection of the orbital electron. This produces a vacancy in an inner shell, which is then filled by an electron from a higher shell, thus emitting photons at the transition energy in the form of an X-ray fluorescence photon or Auger electron.
Rayleigh (or Thompson) scattering is an elastic and coherent form of scattering: the incident and scattered X-ray photons have the same energy and phases. It occurs when low-energy photons interact with the whole atom of the absorber material. As a consequence, the electron shell of the absorber atom begins to oscillate, thus emitting scattered radiation. In Rayleigh scattering, only the direction of propagation is changed through polarization.
Compton scattering is an inelastic and incoherent form of scattering. The X-ray photon collides with a quasi-free electron of the absorber atom. In contrast to to the photoelectric absorption process, it transfers a part of its energy to the electron. If the transmitted energy from the photon is greater than the binding energy of an electron, the atom is ionised, and the photon loses energy. The incident photon with reduced energy is then scattered at a certain scattering angle (Schoerner, 2012).

Photoelectric absorption is dominant in the lower photon energy range (< 100 keV). Compton scattering exceeds the photoelectric absorption for most industrial materials for photons with energy around 150 keV and above. Rayleigh scattering is typically less dominant in the energy ranges relevant for this work (0 keV to 225 keV) (Chantler, 1995).

1.2.2 Estimation and reduction

Different methods are used to estimate scattered radiation, the contribution of which can be simulated. Some analytical methods show good agreement for simpler CT geometries (Kyriakou et al., 2006); however, for complex CT geometries, a more accurate and general way of simulating scattered radiation contribution is to use the Monte Carlo simulation (Ay & Zaidi, 2005; Chan & Doi, 1983; Inanc, 1999).

It has been shown that Monte Carlo simulations with different system configurations are a reliable tool for acquiring information about the possibilities of reducing scattered radiation. This is especially the case for environmental scattering via a CT system redesign (Schuetz et al., 2013).

1.3 Monte Carlo simulation (GATE)

There is a variety of different Monte Carlo simulation tools on the market. They range from dedicated Monte Carlo codes for Positron Emission Tomography (PET) or Single Emission Computerized Tomography (SPECT) to more versatile simulation codes such as GEANT4 (OpenGATE Collaboration, 2021). GEANT4 is used for the simulation of the passage of particles through matter. Its application areas range from high energy to nuclear and accelerator physics to studies in medical and space sciences (CERN Acceleration sciences, 2021). GATE is an advanced open-source software based on the GEANT4 toolkit. It makes use of the well-validated physics models, sophisticated geometry description and powerful visualisation tools of GEANT4 and extends the native command interpreter of GEANT4 to a dedicated scripting mechanism referred to as the macro language (OpenGATE Collaboration, 2021).

1.4 Contribution of this thesis

Research question

How much scattered radiation is produced through physical scattering effects in CT system LuCi, hampering the qualitative and quantitative analysis of CT scans?

Aim

The aim of this bachelor thesis is the analysis and quantification of the scattered radiation contribution in the CT system LuCi, using the Monte Carlo simulation and comparing the results to experimental measurements. The study can be broken down into the following elements:

A_1 Research
- A_1.1 Concept of CT scanners
- A_1.2 Scattered radiation and methods of estimation and reduction

A_2 Simulation of CT system LuCi and estimation of scattered radiation contribution
- A_2.1 Simulation setup
  - A_2.1.1. Definition of source and detector
  - A_2.1.2. Definition of phantom
- A_2.2 Measurements with different combinations of scattering effects

A_3 Experimental estimation of scattered radiation with phantoms

A_4 Comparison of estimated through simulation vs experimentally measured scattered radiation contribution

Hypotheses

Simulating virtual CT scans with the Monte Carlo simulation (GATE) using different phantoms is a promising approach for the accurate estimation of the scattered radiation contribution in the CT scans acquired by LuCi.

H_1 With GATE, the individual physical effects can be turned on and off in a way that allows a differentiation of the total measured scattered radiation into contributions relating to specific physical effects.

H_2 The measured scattered radiation contribution acquired with the GATE simulation is around 8%, as also suggested by preliminary estimates of scattered radiation obtained through the experimental approach.

Methodology

The goal of this thesis is to estimate the contribution of scattered radiation by using different simulation setups. To achieve this objective, the Monte Carlo simulation was chosen because of its implementation in various other studies. This concept has been shown to produce good agreement between measured and simulated X-ray spectra, as well as projections (Miceli, Thierry, Bettuzzi, et al., 2007; Miceli, Thierry, Flisch, et al., 2007). GATE, a GEANT4-based simulation platform which is a toolkit for the simulation of the passage of particles through matter, is used for this thesis. GATE is an open-source Monte Carlo simulation tool, which is widely recognised by the scientific community for its accuracy and validity (Jan et al., 2011). In a further step, experimental measurements using phantoms are planned for comparison.

2 Materials and methods

For the first GATE simulation steps, vGATE was used. vGATE is a virtual machine running on a Ubuntu 64-bit operating system, with GATE 9.0 and further packages preinstalled. It can be downloaded from the OpenGate collaboration website and imported into the VM VirtualBox Manager. As a virtual machine, it can be installed on different operating systems.

vGATE was primarily used for the development of the system setup as well as simulations over a shorter timeframe. To run longer simulations, a workstation with GATE installed was used at the HSLU.

A GATE simulation is split into two parts. Within the first part, the geometry (detector and phantom) and physics processes are defined. Before the second part begins, all the defined characteristics from the first are initialised. Within the second part, the digitiser, source and data output are defined. Finally, the simulation itself is started. The following description of the setup is based on the information acquired from the GATE documentation available at the OpenGate collaboration website (see Appendix B.1).

2.1 General simulation setup

Figure 2 depicts the coordinate system, general setup and placement of the components. For the simulations, the detector is placed in the xy-plane and translated along the z-axes in the positive direction. The source is also translated along the x-axes, however in the negative direction and, strictly speaking, also situated in the xy-plane. The cone beam itself is facing the detector and the phantom. The phantom is placed between the source and the detector. For different simulations, it can be translated along the x-axes, nearer to or farther from the detector. The cabinet surrounds the whole system and consists of a source, a phantom, a detector and additional parts such as the granite blocks, detector holder and object holder.

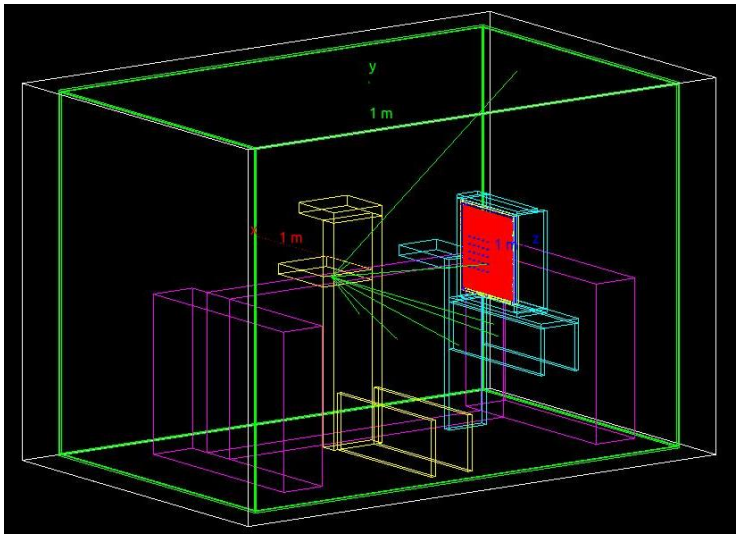

Figure 2: Coordination system and object placement

2.1.1 Visualisation and verbosity

With the visualisation settings in GATE, different output options can be chosen. When running a script, for example, the simulation setup can be viewed in a specific OpenGL viewer.

The verbosity can be set with values from 0 to 2, which define the amount of printing in the command window of a specific aspect.

2.1.2 Geometry

For the creation of individual volumes, a material database must be defined. The material database consists of the definition of all elements from which different material compositions are created. The location of the material database must be specified with the following command:

/gate/geometry/setMaterialDatabase *GateMaterials.db*

The download of the GATE software contains a material database with the most commonly used elements and some predefined materials. The file is named GateMaterials.db and was used as a basis for the simulations conducted as part of this project. Further materials, such as diamond, graphite, caesium iodine (CsI), granite and steel, were also defined for this project. Apart from CsI, granite and steel, which were implemented in the simulations, the other materials were only used for testing purposes.

The file containing the predefined material database can be found in the subfolders of the GATE simulation examples, generally in a subfolder called “data”. Similarly, for the simulations within this project, the material database (GateMaterials.db) is also saved in a subfolder called “data” within the folder structure of each simulation.

The general concept of the creation of volumes is that there is the main volume called “world” and sub-volumes called “daughter”.
Three rules apply for the creation of volumes (OpenGATE Collaboration, 2021):

- A volume which is located inside another must be its daughter.
- A daughter must be fully included in its mother.
- Volumes must not overlap.

2.1.2.1 Detector

To acquire information regarding particle interaction, a detector must be defined as a specific system. Different systems are available, such as scanner/PETscanner, CTscanner, cylindrical PET, SPECThead and many more. For the current project, the detector system used was the CTscanner. Attached to the use of the CTscanner system is a corresponding correlation of the mother/daughter volumes, as shown in Table 1.

Table 1: CTscanner system description (OpenGATE Collaboration, 2021)

System	Component and Shape		Attach Keyword Argument	Depth for readout segmentation	Available Outputs
CTscanner	module	box	“module”	1	Raw Data, ASCII, ROOT
	cluster	box	“cluster 0…2”	2	
	pixel	box	“pixel 0…2”	3	

For this project, two levels of flat panel detectors were created, based on the properties of the flat panel detector (XRD 4343CT) used by the CT system LuCi. For the recreation of the simplified versions of the detector, the datasheet available at the homepage of Varex Imaging was used.

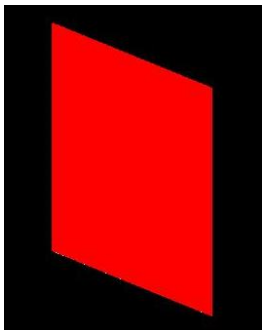

Figure 3: Basic flat panel detector

Figure 3 shows the basic version, consisting only of a 432 x 432 x 1 mm volume (module/cluster) containing 1 mm CsI cubes (pixel) throughout the volume. In regard to simulation performance aspects, the pixel size of 1 x 1 mm^2 was chosen. The main purpose of the basic flat panel detector was to run different tests at the beginning of the project.

Figure 4 shows the more sophisticated version. The size of the whole detector is 470 x 470 x 32 mm. Figure 5 and Figure 6 show the individual parts in explosion visualisation: whole detector (white), front panel (purple), scintillator (red), photodetector (blue) and housing (yellow).

The whole detector (white) is the mother volume, and all the other parts are its daughter. Therefore, they are fully included in the whole detector. The specifications for the individual parts are shown in Table 2. A notable fact is that the housing essentially encases the whole detector (the back and all the sides). The photodetector volume is defined as the volume within the mother volume which is not filled by other parts. Within the scintillator, 1 mm CsI cubes are placed throughout the whole volume, as in the basic detector version. It is rumoured that a tungsten layer is placed between the scintillator and the photodetector to shield the electronics. For this detector setup, it was decided to stick to the parts described in the datasheet.

Table 2: Sophisticated flat panel detector – specifications

Part	Size (mm)	Material
Front panel	466 x 466 x 1	Epoxy
Scintillator	432 x 432 x 1	CsI
Photodetector: Back panel Left/right-hand panel Top/bottom panel	 432 x 432 x 28 466 x 29 x 17 432 x 29 x 17	Silicon
Housing: Back panel Left/right-hand panel Top/bottom panel	 466 x 466 x 2 470 x 32 x 2 466 x 32 x 2	Aluminium

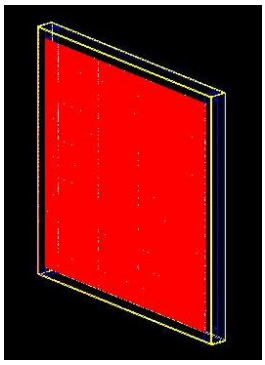

Figure 4: Sophisticated flat panel detector

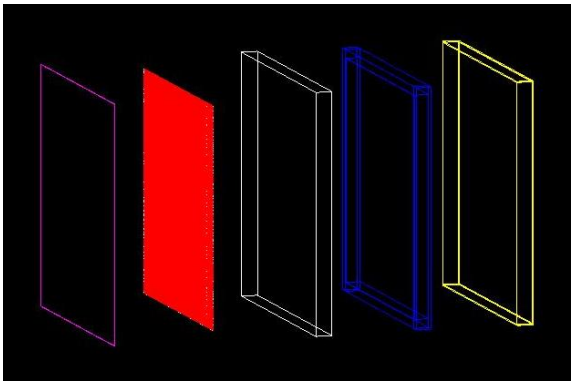

Figure 5: Sophisticated flat panel detector – exploded view (wireframe)

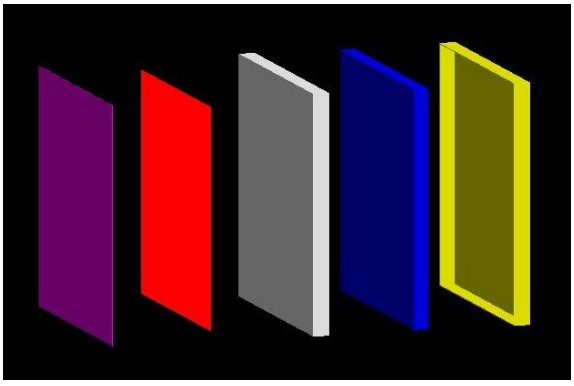

Figure 6: Sophisticated flat panel detector – exploded view (solid)

2.1.2.2 Phantom

During the development of the GATE simulation setup, a variety of phantoms was used for different purposes. All were cylindrically shaped, but they varied in dimensions and material. The list, with specifications, is presented in Table 3.

Table 3: Phantom – specifications

Phantom	Diameter (mm)	Height (mm)	Spacing (mm)	Material
Vertical cylinder	100	100	-	Aluminium Tungsten
Horizontal cylinder	100	100	-	Aluminium Tungsten
	10	10	-	Lead Tungsten
Scatter grid (5 by 5 grid)	5	10	40 (centre to centre)	Lead

Principally for the testing of the different data output options (see section 2.1.7), sole cylinders in vertical or horizontal orientation were used. The lateral area of a cylinder in vertical orientation (see Figure 7 and Figure 8) faces the detector, while the base of a horizontal cylinder (see Figure 9 and Figure 10) faces the detector.

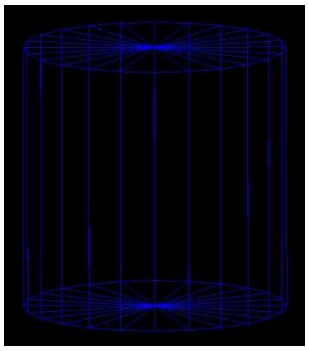

Figure 7: Vertical cylinder (wireframe)

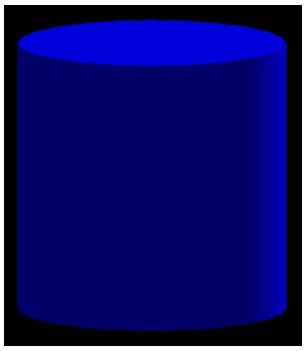

Figure 8: Vertical cylinder (solid)

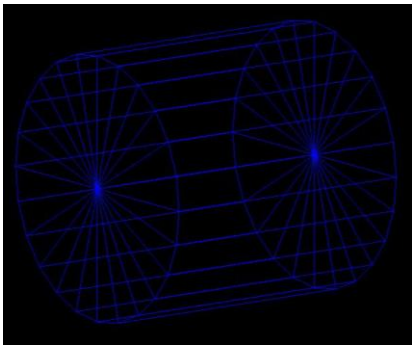

Figure 9: Horizontal cylinder (wireframe)

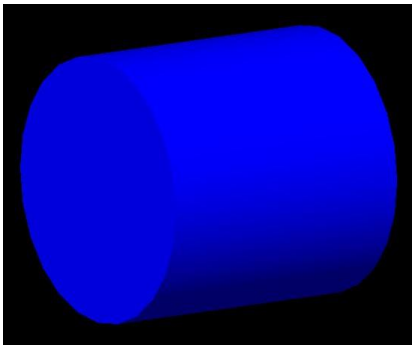

Figure 10: Horizontal cylinder (solid)

For the simulation and measurement of the scattered radiation for different system setups, a scatter grid was used, as depicted in Figure 11 and Figure 12, consisting of a 5x5 matrix of identical cylinders.

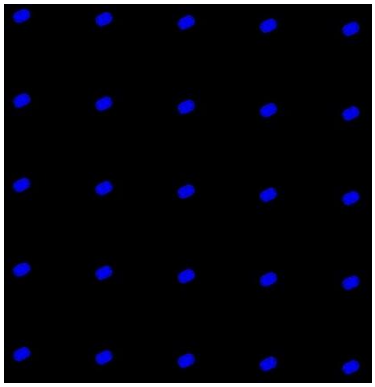

Figure 11: Scatter grid (wireframe)

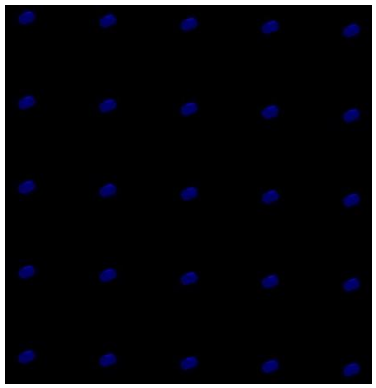

Figure 12: Scatter grid (solid)

2.1.2.3 Cabinet

The whole CT system is encased in a cabinet. Within the simulation setup, the cabinet is represented by six walls, as can be seen in Figure 13 and Figure 14. The dimensions of the cabinet were measured directly at LuCi and are documented in Appendix B.2.1. During the development of the simulation setup, two cabinet versions were used (see Table 4). The first version consists of one lead layer with the same thickness for all sides, while the second was a steel-lead-steel "sandwich", with the lead layer varying in thickness depending on the side. The steel was defined as a material (see section 2.1.2) consisting of iron (73.2%), carbon (0.8%), chromium (18%) and nickel (8%), based on 304 stainless steel.

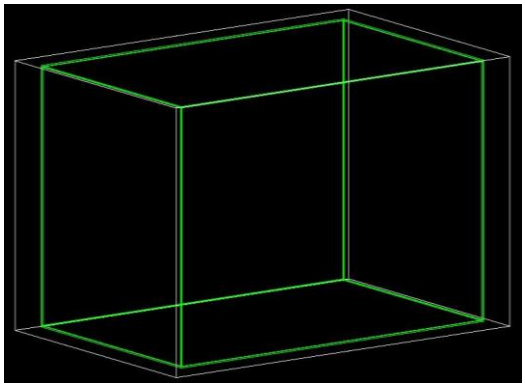

Figure 13: Cabinet (wireframe)

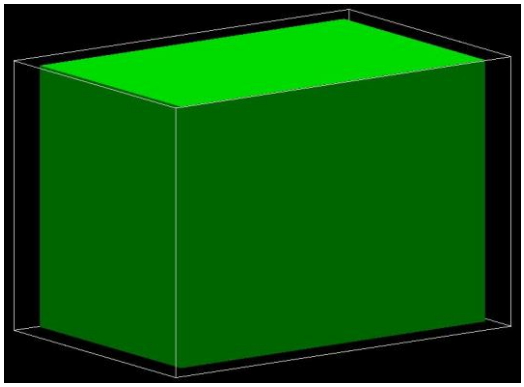

Figure 14: Cabinet (solid)

Table 4: Cabinet – specifications

Cabinet version	Wall placement	Thickness (mm)	Material
1-Layer	All	10	Lead
Sandwich	Front	4 / 16 / 4	Steel / Lead / Steel
	Back	4 / 12 / 4	
	Right	4 / 12 / 4	
	Left	4 / 12 / 4	
	Bottom	4 / 12 / 4	
	Top	4 / 12 / 4	
	Door (not implemented)	4 / 20 / 4	

2.1.2.4 Granite

The dimensions of the granite blocks were measured in the CT system LuCi and are documented in Appendix B.2.1. They were placed in the simulation setup as depicted in Figure 15 and Figure 16. The granite was defined as a material (see section 2.1.2) consisting of SiO2 (80%) and Al2O3 (20%).

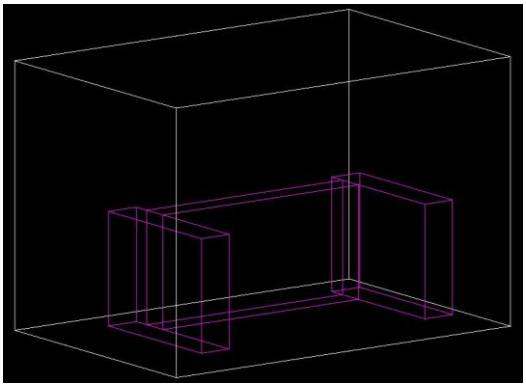

Figure 15: Granite (wireframe)

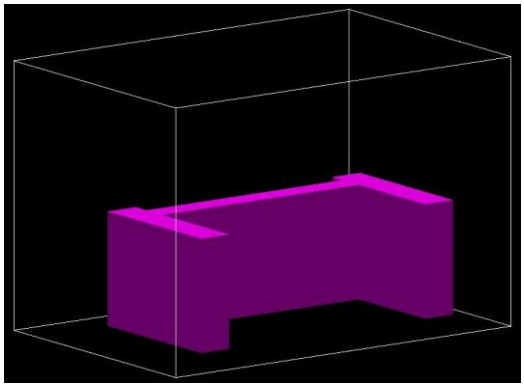

Figure 16: Granite (solid)

2.1.2.5 Detector holder

The detector holder is portrayed in Figure 17 and Figure 18, and all parts are made from aluminium. Its dimensions were taken from LuCi and are documented in Appendix B.2.2. Figure 19 and Figure 20 show the detector holder, including the actual detector (see section 2.1.2.1). The whole detector holder setup was constructed to allow its easy translation along the z-axes.

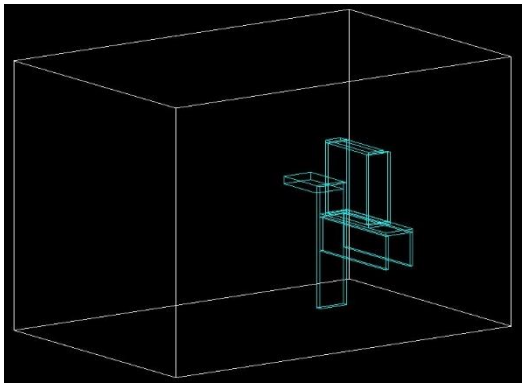

Figure 17: Detector holder (wireframe)

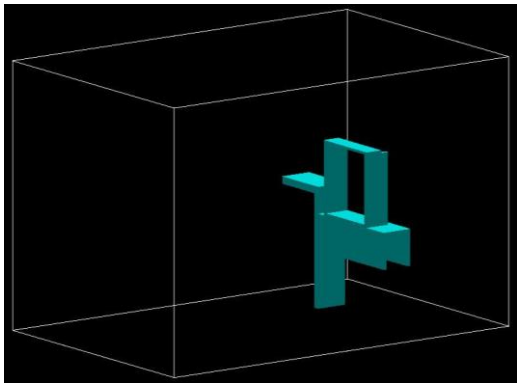

Figure 18: Detector holder (solid)

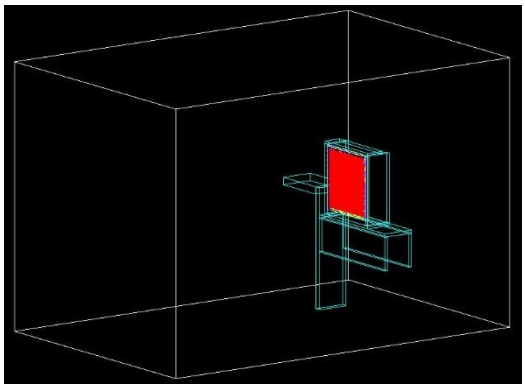

Figure 19: Detector holder and detector (wireframe)

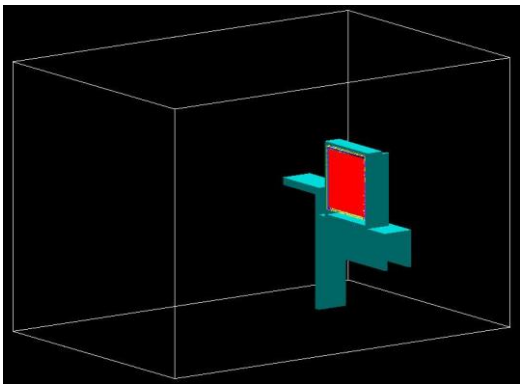

Figure 20: Detector holder and detector (solid)

2.1.2.6 Object holder

The dimensions of the object holder were also taken from the CT system LuCi and documented in Appendix B.2.3. Its placement within the simulation setup is illustrated in Figure 21 and Figure 22. All parts were made from aluminium. Its construction allows the easy translation of the whole object holder along the z-axes.

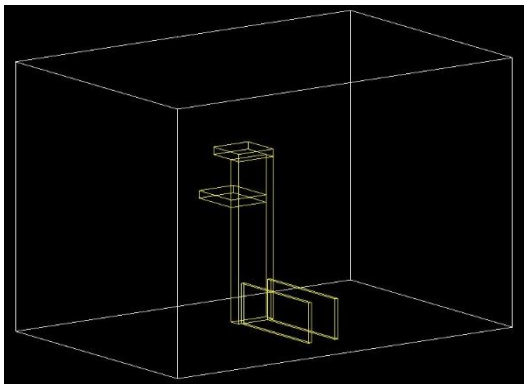

Figure 21: Object holder (wireframe)

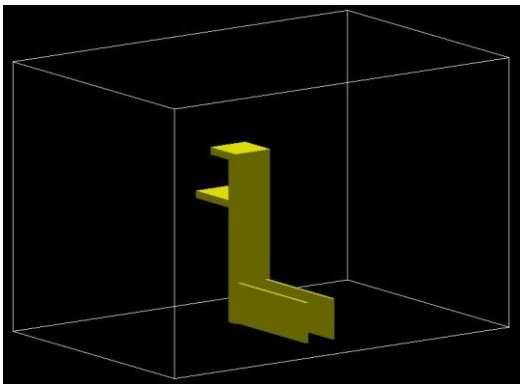

Figure 22: Object holder (solid)

2.1.3 Physics processes

GATE offers the option to choose between a predefined physics list or build a new one by adding individual physics processes. Physics lists can be added with the following command:

/gate/physics/addPhysicsList *emstandard_opt3*

For the simulations within this project, the physics list "emstandard_opt3" was used. This list includes the most important physics processes for gamma particles and electrons, such as the photoelectric effect, Compton scattering, Rayleigh scattering, pair production, multiple scattering, electron ionisation and bremsstrahlung. All the defined physics processes, as well as the defined modules, can be found in the source code of GEANT4.

It was further planned to make use of the option of building a specified physics list due to the possibility of activating and deactivating different scattering effects and, therefore, the option of simulating the scattered radiation with different configurations. After this method had been evaluated, it was decided not to use it because the results of the energy deposition acquired differed between the predefined and self-defined physics list (see section 2.1.9 and section 3.1.1 for the methodology and results).

To avoid infrared divergence, a cut length must be set for all particles. The energy deposition for a variety of cut lengths for gamma particles and electrons was simulated (see section 2.1.10 and section 3.1.2 for the methodology and results). For further simulations, it was set to 0.1 µm for all particles.

2.1.4 Initialize

After the definition of the geometry and the physics processes, the initialisation is started with the following command:

/gate/run/initialize

After the initialisation, it is no longer possible to modify the physics list or modify or add new volumes.

2.1.5 Digitiser

The digitiser is used to mimic the signal processing of a real detector. The detected hits are processed by the defined signal processing chain, which leads to the output of a pulse, which is the physical observable seen from the detector and also called a single. Different modules for the signal processing chain are available, principally Adder, which adds up all the hits within a crystal to a pulse, and Readout, which regroups pulses to one pulse per group of sensitive detectors.

To obtain any information about the interaction of particles with matter (hits), it is important to connect a detector volume (which must be part of the specified detector system) as well as a phantom volume to a sensitive detector. The detector must be attached to the so-called CrystalSD and the phantom to the PhantomSD. It is not possible to connect the same volume to both sensitive detectors. A volume can be connected with the following command:

/gate/*pixel*/attachCrystalSD

/gate/*Cylinder*/attachPhantomSD

2.1.6 Source

GATE presents the option to use different source types as well as different ways to define the energy distribution. The source type chosen for this project is called gps (general purpose source). For the definition of the energy distribution, the option UserSpectrum was chosen, for which a histogram (txt-file) of the source spectrum can be given as an input. The source spectra were generated before the start of this thesis via simulations in GATE. A short description of the simulation setup can be found in section 2.1.6.1. As an input for the UserSpectrum, a histogram generated with an acceleration voltage of 160 kV and a 6.5 µm thick tungsten target was chosen (see Figure 23).

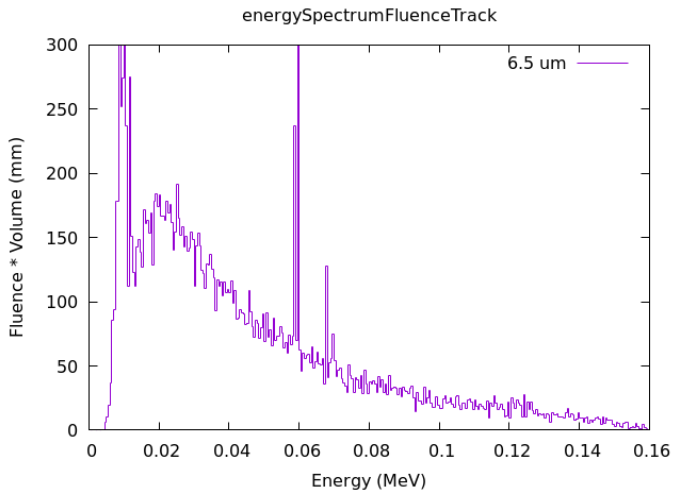

Figure 23: Source spectrum 160 kV acceleration voltage, 6.5 µm thick W target

The source itself is a cone beam source with a focal point of 5 µm radius and a gamma distribution along the x-axes with a cone beam angle of 30° (Figure 24). Figure 25 shows that a nearly complete irradiation of the sensitive detector (red) along the y- and z-axes of the detector area is achieved.

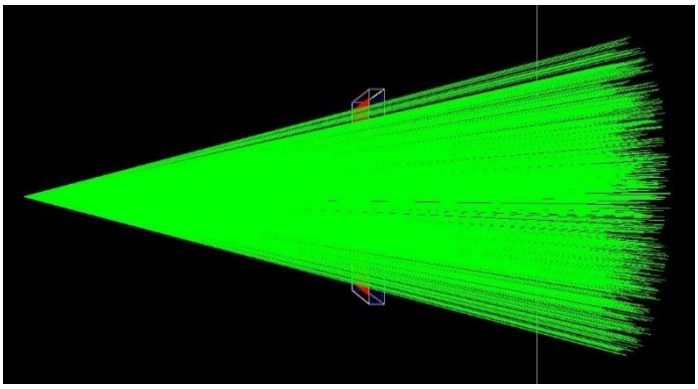

Figure 24: Source – cone beam

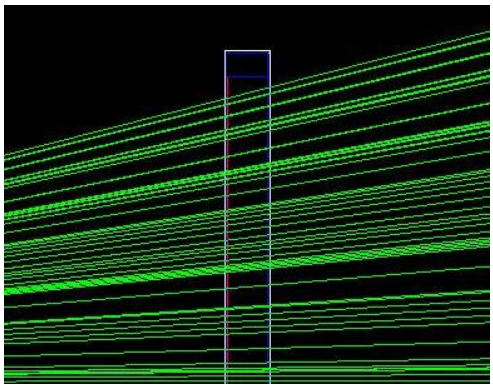

Figure 25: Source – top half of detector

After the addition of the cabinet, during the development of the simulation setup, the cone beam angle was increased to 135° in order to take the scattered radiation of the cabinet into account.

2.1.6.1 Source spectrum

The simulation for the source spectra was conducted before the start of this thesis. The spectra were simulated for different configurations of tungsten target thickness (1.0, 3.5, 6.5, 9.0 µm) as well as different acceleration voltages (40, 80, 120, 160, 200, 240 kV). Figure 26 shows the source spectrum for a simulation with 160 kV acceleration voltage and varying target thickness, and Figure 27 shows the results of a simulation with a 6.5 µm tungsten target and varying acceleration voltages. The source used in LuCi is an [XWT-225 TCHE+].

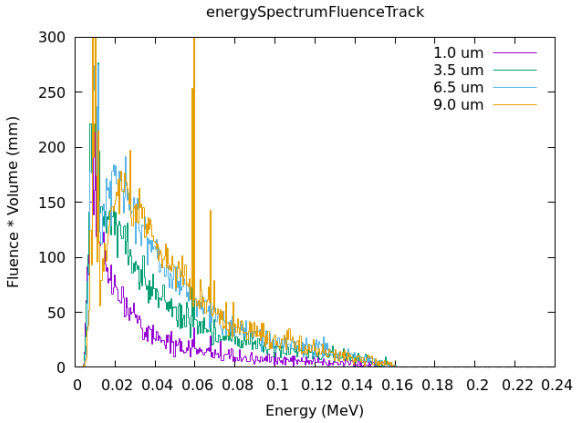

Figure 26: Source spectrum 160 kV with 1.0, 3.5, 6.5, 9.0 µm thick W target

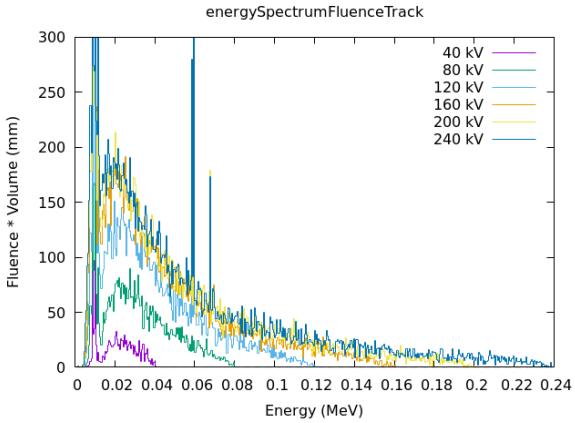

Figure 27: Source spectrum 6.5 µm thick W target with 40, 80, 120, 160, 200, 240 kV acceleration voltage

The simulation setup itself can be seen in Figure 28. It consists of a mono-energy electron source directed towards the target to create gamma particles. The electrons are coloured red and the gamma particles are shown in green.

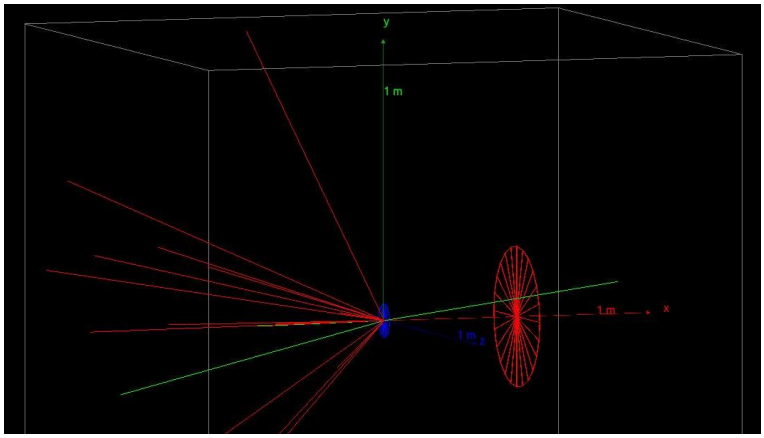

Figure 28: Source spectrum – simulation setup

The geometrical setup in Figure 29 consists of a tungsten target (blue) with a carbon target (yellow) barely visible behind it and a detector plane (red). The specifications are reported in Table 5.

Table 5: Source spectrum setup – specifications

Part	Size r, h (mm)	Material
Target C	8, 0.3	Carbon
Target W	60, 0.0065	Tungsten
Detector plane	250, 1	Vacuum

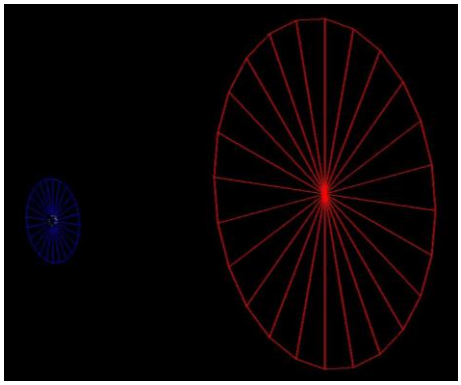

Figure 29: Spectrum simulation – target and detector plane

2.1.7 Data output

The GATE software offers several different options for data as well as data formats. Most data can be saved in ASCII, Raw and Root format. Generally, it can be differentiated between the output described in section 2.1.7.1 and the actor described in section 2.1.7.2. The former must be defined after the initialisation whereas the latter has to be defined before the initialisation.

Interference between these data output types was observed. If both outputs were activated, only the actor data output worked. Even though other output files could be created, they contained no data. It is assumed that the interference is bilateral and that actor data output is always the one functioning because, from a chronological point of view, it is the first to be defined. Therefore, it is important to deactivate the unwanted data output (comment out macro file execution).

If a simulation with both data output types is required, a proposed solution is to set the EngineSeed manually, thereby making it possible to run a simulation twice with the same particle output of the source. For further information, see section 2.1.8.

For all data outputs, a gamma particle filter was set. The filter was attached to the detector volume "module", so that only gamma particles hitting the volumes described in section 2.1.2.1 were recorded.

2.1.7.1 Output

Different types of data outputs are grouped together under the title "output". The data outputs discussed below were studied in detail accurately and partially used for simulations.

Root output

The root output contains up to three trees (Hits, Singles, Coincidences) in which several variables are stored. For example, information about Compton and Rayleigh scattering is stored for the volumes connected to PhantomSD and CrystalSD. The root files can be opened with the TBrowser, which is a graphical user interface to visualise the produced simulation data.

To reduce simulation time and safe space, only the required trees should be enabled. The most relevant trees are the singles tree and, if necessary, the hits tree (adds substantial simulation time and output data size).

Image CT output

The Image CT output is a binary matrix that stores the number of singles per pixel. The output resolution – respectively, the pixel size – is given through the geometrical aspects of the detector setup.

The raw image file with a .dat ending can be opened with an image viewer such as Fiji. In Fiji, the import of a raw file must be chosen, and parameters must be set. The image type is a "32-bit Real". The pixel height and width must be set as predefined in the setup of the detector geometry, and the "Little-endian byte order" box has to be checked.

2.1.7.2 Actor

Actors are tools to interact with the simulation while it is running. Some can interact by changing the simulation actively while others behave more passively and only collect information during the simulation. The output data format can range from ASCII over Raw to Root and is specific for each actor. For some actors, only one data format at a time is possible, while others can save the same output as different output formats.

Simulation statistic

The simulation statistics actor counts the number of steps, tracks, events and runs in the simulation. It can be attached to a volume. Therefore, it only counts the abovementioned interactions for the chosen volume. The gathered data is saved in a text file.

Energy spectrum

The energy spectrum actor builds one root file containing different histograms. Additionally, the data of each histogram can be saved as a text file. Histogram types included range from an energy deposition spectrum to energy fluence spectrum and number of particles spectrum.

For most of these histograms, the number of bins and energy range can be set individually. Additionally, by introducing a filter to the actor, only a specific particle can be taken into account for the histogram outputs.

Dose measurement

The dose measurement actor builds 3D images of the energy deposition (MeV), the dose deposition (Gy) and the number of hits in the attached volume. For the energy deposition as well as the energy dose, additional image outputs (uncertainty, squared) can be enabled. The output itself can be ASCII, root or MetaImage. The MetaImage is a combination of an mhd and raw file and can be opened with image visualisation software such as Fiji.

The resolution of the image output can be changed. It can be set to the same pixel size as in the definition of the detector geometry or to a smaller pixel size but never to a bigger one.

2.1.8 Acquisition

The final step is the definition of the acquisition. A random engine, an engine seed and the total number of primary particles must be set. Three different random engines are available. The default option is called MersenneTwister, which was used throughout this project. The engine seed can be set to auto for a new seed for each time GATE is run or to a specific value to have the same seed for all simulations. If simulations with the same source but a different setup were run, the source was set to “123456” in order to remove variance from the output. When multiple simulations were run with the same setup, the seed was set to a specific value, which was changed for each simulation. The total number of particles varied between 1e5 and 2e8, depending on the goal of the individual simulation.

The acquisition is started and the simulation closed after it finishes with the following commands:

```
/gate/application/start
exit
```

2.1.9 Physics processes

As described in section 2.1.3, there are two options for the setup of the physics processes: choosing a predefined physics list or defining a specific one by adding individual physics processes. To compare self-defined physics lists to the "emstandart_opt3" chosen from the predefined physics lists, the two simulation setups in the following sections were used. Section 2.1.9.1 describes the simulation setup for a general comparison of the two mentioned physics lists, and section 2.1.9.2 presents further analysis with different particle filters. For the results, see section 3.1.1.

2.1.9.1 Physics lists

General information on the simulation setup is presented in Table 6.

Table 6: Physics processes (physics lists) – general information on setup

Parameter	Value
Primary particles	1e5
Engine seed	123456 (fixed)
Source to detector distance (SDD)	784 mm

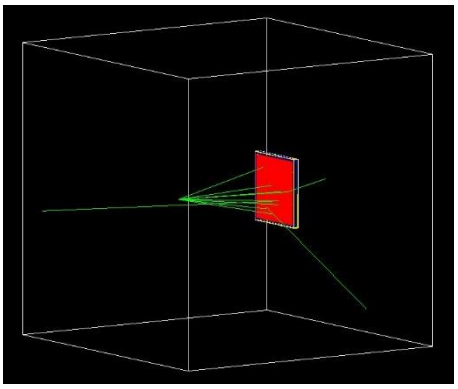

Figure 30: Physics processes (physics lists) – simulation setup

Geometry

On the geometrical side, the simulation setup consisted only of a detector; no other physical parts were simulated (see Figure 30). The setup of the used detector is described in section 2.1.2.1. It is visualised in Figure 4 to Figure 6, and its specifications are presented in Table 2.

Source

For the X-ray source, a source spectrum with 160 kV acceleration voltage and 6.5 µm thick W target was used (see section 2.1.6). The full angle of the cone beam was set to 30°, irradiating nearly the whole detector horizontally and vertically for the set SDD.

Physics processes

For the predefined physics list, the "emstandart_opt3" with a cut length of 0.1 µm for all particles was used. Within the self-defined physics list, the particles and physics processes presented in Table 7 were chosen. The cut length was also set to 0.1 µm for all particles.

Table 7: Physics processes (physics lists) – particles and physical effects

Particle	Physical effect
Gamma	Photoelectric effect
	Compton scattering
	Rayleigh scattering
	Pair production
Electron	Multiple scattering
	Electron ionisation
	Bremsstrahlung

Data output

For the output, the actor macro file was used, which contains the EnergySpectrumActor. It produces a text and root file containing the energy deposition spectrum for each simulation, allowing a comparison and further analysis of the histograms.

2.1.9.2 Particle filters

General information on the simulation setup can be seen in Table 8.

Table 8: Physics processes (filter) – general information on setup

Parameter	Value
Primary particles	1e5
Engine seed	auto (random)
Source to detector distance (SDD)	784 mm

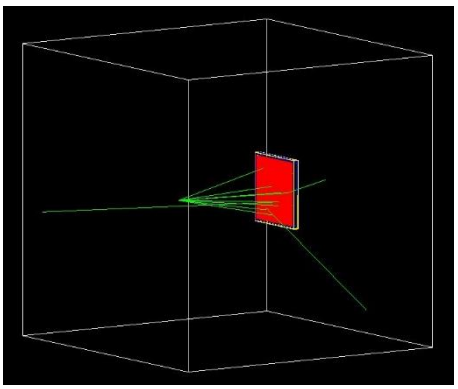

Figure 31: Physics processes (filter) – simulation setup

Geometry

The simulation setup from the geometrical side consisted only of a detector; no other physical parts were simulated (see Figure 31). The setup of the used detector is described in section 2.1.2.1. It is visualised in Figure 4 to Figure 6, and its specifications are presented in Table 2.

Source

For the X-ray source, the source spectrum with 160 kV acceleration voltage and 6.5 µm thick W target was used (see section 2.1.6). The full angle of the cone beam was set to 30°, irradiating nearly the whole detector horizontally and vertically for the set SDD.

Physics processes

For the predefined physics list, the "emstandart_opt3" with a cut length of 0.1 µm for all particles was used. Within the self-defined physics list, the particles and physics processes presented in Table 9 were chosen. The cut length was also set to 0.1 µm for all particles.

Table 9: Physics processes (filter) – particles and physical effects

Particle	Physical effect
Gamma	Photoelectric effect
	Compton scattering
	Rayleigh scattering
	Pair production
Electron	Multiple scattering
	Electron ionisation
	Bremsstrahlung

Data output

For the output, the actor macro file was used, which contains the EnergySpectrumActor. It produces a text and root file containing the energy deposition spectrum for each simulation, allowing a comparison and further analysis of the histograms. Four simulations were performed with a different filter setting (no filter, gamma filter, electron filter, ion filter) for each.

2.1.10 Production threshold

As described in section 2.1.3, a production threshold, under which no secondary particles are produced, must be set for all particles. It is defined as a cut length called CutInRegion. This value was varied to analyse its influence on the general simulation setup. For the results, see section 3.1.2.

General information on the simulation setup can be seen in Table 10.

Table 10: Production threshold – general information on setup

Parameter	Value
Primary particles	1e5
Engine seed	auto (random)
Source to detector distance (SDD)	784 mm

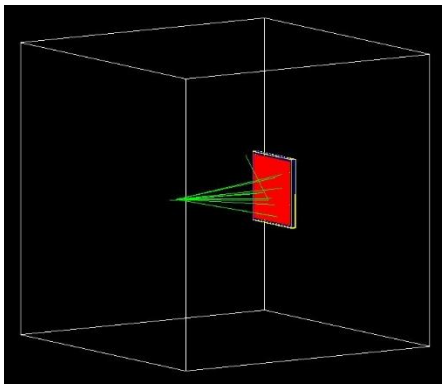

Figure 32: Production threshold – simulation setup

Geometry

The geometrical simulation setup consisted only of a detector (see Figure 32). No phantom, cabinet or other physical parts were simulated. The setup of the used detector is described in section 2.1.2.1. It is visualised in Figure 4 to Figure 6, and its specifications are presented in Table 2.

Source

For the X-ray source, the source spectrum with 160 kV acceleration voltage and 6.5 µm thick W target was implemented (see section 2.1.6). The full angle of the cone beam was set to 30°, irradiating nearly the whole detector horizontally and vertically for the set SDD.

Physics processes

As a physics list, the predefined option called “emstandart_opt3” was used for the simulations. As a baseline, a cut length of 0.1 µm for all particles was used. Additionally, the cut length was set to 1 µm, 10 µm, 100 µm and 1 mm individually for gammas and electrons.

Data output

For the output, the actor macro file, which contains the EnergySpectrumActor, was used. It produces a text and root file containing the energy deposition spectrum for each simulation, allowing a comparison and further analysis of the histograms.

2.2 Simulated approach (GATE)

For the simulations of scattered radiation, two simulation rounds were performed. For the first round, the number of primary particles was set to 1e8, and for the second round, they were doubled to 2e8. In each round, different geometrical system configurations were simulated to acquire the scatter influence of a specific geometrical part. An example simulation macro file setup can be seen in Appendix A.

2.2.1 Configuration (p)

This section describes the system setup for the simulations with only a phantom. The results are documented in section 3.2.1. General information on the simulation setup is presented in Table 11.

Table 11: Configuration (p) – general information on setup

Parameter		Value
Primary particles	1st round 2nd round	1e8 2e8
Engine seed	1st round 2nd round	1 digit → xxxxxx | e.g. simulation 8 → 888888 2 digits → 1xxxxxx | e.g. simulation 12 → 1222222 1 digit → xxxxxxx | e.g. simulation 7 → 7777777 2 digits → 1xxxxxxx | e.g. simulation 10 → 10000000 (note: x → last digit of simulation)
Source detector distance (SDD)		1000 mm
Object detector distance (ODD)		50 mm
X-axes (source, object, detector alignment)		0 mm

Geometry

The simulation setup from a geometrical viewpoint consisted of a detector and phantom (see Figure 33). The setup of the used detector is described in section 2.1.2.1. It is visualised in Figure 4 to Figure 6, and its specifications are presented in Table 2. The phantom (scatter grid) is described in section 2.1.2.2 and visualised in Figure 11 and Figure 12.

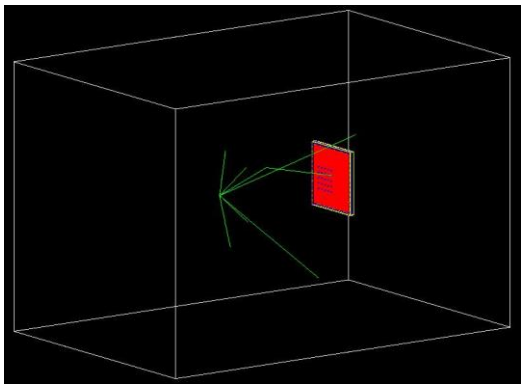

Figure 33: Configuration (p) – simulation setup

The detector, source and phantom are placed at the world's centre (x-axes), which does not correspond with the actual placement in LuCi.

Source

For the X-ray source, the source spectrum with 160 kV acceleration voltage and 6.5 µm thick W target was used (see section 2.1.6). The full angle of the cone beam was set to 135°.

Physics processes

As a physics list, the predefined option called "emstandart_opt3" was used for the simulations. The production threshold was set to a cut length of 0.1 µm for all particles.

Data output

The actor macro file, which contains the DoseActor, was used for the output. It produces a MetaImage, a combination of an mhd and a raw file, containing the energy deposition per pixel. The Image was set to a resolution of 864 by 864 pixels (see section 2.1.7.2). The resulting image files were further analysed with a Fiji macro (see section 2.2.8).

2.2.2 Configuration (p + cab)

This section describes the system setup for the simulations with a phantom and a cabinet surrounding the whole system. The results are documented in section 3.2.2. General information on the simulation setup is presented in Table 12.

Table 12: Configuration (p + cab) – general information on setup

Parameter		Value
Primary particles	1st round 2nd round	1e8 2e8
Engine seed	1st round 2nd round	1 digit → xxxxxx | e.g. simulation 8 → 888888 2 digits → 1xxxxxx | e.g. simulation 12 → 1222222 1 digit → xxxxxxx | e.g. simulation 7 → 7777777 2 digits → 1xxxxxxx | e.g. simulation 10 → 10000000 (note: x → last digit of simulation)
Source detector distance (SDD)		1000 mm
Object detector distance (ODD)		50 mm
X-axes (source, object, detector alignment)		0 mm

Geometry

The geometrical simulation setup for this part consisted of a detector, phantom and cabinet (see Figure 34). The chosen detector is detailed in section 2.1.2.1. It is visualised in Figure 4 to Figure 6, and its specifications are presented in Table 2. The phantom (scatter grid) is described in section 2.1.2.2 and visualised in Figure 11 and Figure 12. For the cabinet, the 1-layer version (see Table 4) was used, as described in section 2.1.2.3.

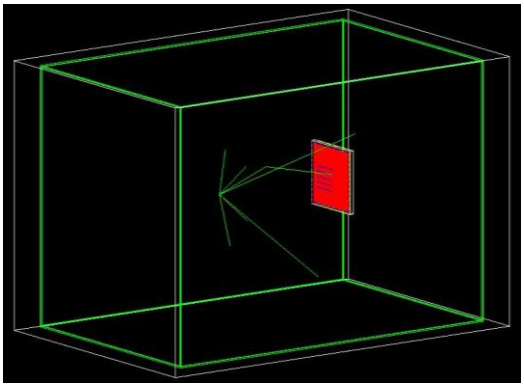

Figure 34: Configuration (p + cab) – simulation setup

The detector, source and phantom are placed at the world's centre (x-axes), which does not correspond with the actual placement in LuCi.

Source

For the X-ray source, the source spectrum with 160 kV acceleration voltage and 6.5 µm thick W target was used (see section 2.1.6). The full angle of the cone beam was set to 135°.

Physics processes

For the simulation the predefined physics list called "emstandart_opt3" was implemented. The production threshold was set to a cut length of 0.1 µm for all particles.

Data output

For the output, the actor macro file was used, which contains the DoseActor. It produces a MetaImage, a combination of an mhd and a raw file, containing the energy deposition per pixel. The Image was set to a resolution of 864 by 864 pixels (see section 2.1.7.2). The resulting image files were further analysed with a Fiji macro (see section 2.2.8).

2.2.3 Configuration (p + gran)

This section details the system setup for the simulations with a phantom and the granite blocks. The results are documented in section 3.2.3. General information on the simulation setup is presented in Table 13.

Table 13: Configuration (p + gran) – general information on setup

Parameter		Value
Primary particles	1st round 2nd round	1e8 2e8
Engine seed	1st round 2nd round	1 digit → xxxxxx | e.g. simulation 8 → 888888 2 digits → 1xxxxxx | e.g. simulation 12 → 1222222 1 digit → xxxxxxx | e.g. simulation 7 → 7777777 2 digits → 1xxxxxxx | e.g. simulation 10 → 10000000 (note: x → last digit of simulation)
Source detector distance (SDD)		1000 mm
Object detector distance (ODD)		50 mm
X-axes (source, object, detector alignment)		0 mm

Geometry

The setup for this specific simulation consisted of a detector, phantom and granite blocks (see Figure 35). The detector used is described in section 2.1.2.1. It is visualised in Figure 4 to Figure 6, and its specifications are presented in Table 2. The phantom (scatter grid) is described in section 2.1.2.2 and visualised in Figure 11 and Figure 12. The granite blocks are described in section 2.1.2.4.

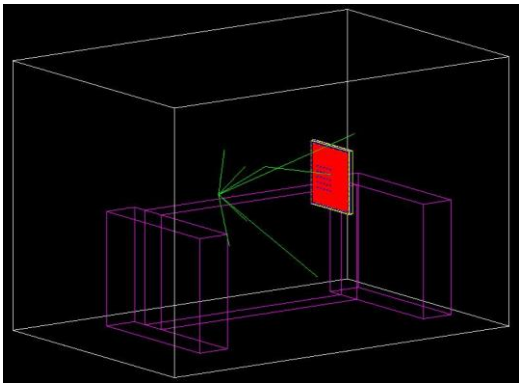

Figure 35: Configuration (p + gran) – simulation setup

The detector, source and phantom are placed at the world's centre (x-axes), which does not correspond with the actual placement in LuCi.

Source

For the X-ray source, the source spectrum with 160 kV acceleration voltage and 6.5 µm thick W target was used (see section 2.1.6). The full angle of the cone beam was set to 135°.

Physics processes

As a physics list, the predefined option called "emstandart_opt3" was used. The production threshold was set to a cut length of 0.1 µm for all particles.

Data output

For the output, the actor macro file was used, which contains the DoseActor. It produces a MetaImage, a combination of an mhd and a raw file, containing the energy deposition per pixel. The Image was set to a resolution of 864 by 864 pixels (see section 2.1.7.2). The resulting image files were further analysed with a Fiji macro (see section 2.2.8).

2.2.4 Configuration (p + cab + gran)

The system setup for the simulations with a phantom, a cabinet and the granite blocks is described below. The results are documented in section 3.2.4. General information on the simulation setup is presented in Table 14.

Table 14: Configuration (p + cab + gran) – general information on setup

Parameter		Value
Primary particles	1st round 2nd round	1e8 2e8
Engine seed	1st round 2nd round	1 digit → xxxxxx | e.g. simulation 8 → 888888 2 digits → 1xxxxxx | e.g. simulation 12 → 1222222 1 digit → xxxxxxx | e.g. simulation 7 → 7777777 2 digits → 1xxxxxxx | e.g. simulation 10 → 10000000 (note: x → last digit of simulation)
Source detector distance (SDD)		1000 mm
Object detector distance (ODD)		50 mm
X-axes (source, object, detector alignment)		0 mm

Geometry

The simulation setup from the geometrical side consisted of a detector, phantom, cabinet and granite blocks (see Figure 36). The detector setup is described in section 2.1.2.1. It is visualised in Figure 4 to Figure 6, and its specifications are presented in Table 2. The phantom (scatter grid) is described in section 2.1.2.2 and visualised in Figure 11 and Figure 12. For the cabinet, the 1-layer version (see Table 4) was used as described in section 2.1.2.3. The granite blocks are described in section 2.1.2.4.

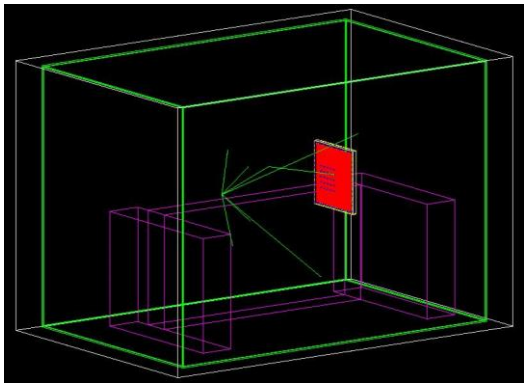

Figure 36: Configuration (p + cab + gran) – simulation setup

The detector, source and phantom are placed at the world's centre (x-axes), which does not correspond with the actual placement in LuCi.

Source

For the X-ray source, the source spectrum with 160 kV acceleration voltage and 6.5 µm thick W target was used (see section 2.1.6). The full angle of the cone beam was set to 135°.

Physics processes

As a physics list, a predefined option called "emstandart_opt3" was used for the simulations. The production threshold was set to a cut length of 0.1 µm for all particles.

Data output

For the output, the actor macro file was used, which contains the DoseActor. It produces a MetaImage, a combination of an mhd and a raw file, containing the energy deposition per pixel. The Image was set to a resolution of 864 by 864 pixels (see section 2.1.7.2). The resulting image files were further analysed with a Fiji macro (see section 2.2.8).

2.2.5 Configuration (p + cabs + gran)

This section details the system setup for the simulations with a phantom, a cabinet and the granite blocks. The results are documented in section 3.2.5. General information on the simulation setup is presented in Table 15.

Table 15: Configuration (p + cabs + gran) – general information on setup

Parameter		Value
Primary particles	1st round	2e8
Engine seed	1st round	1 digit → xxxxxxx | e.g. simulation 7 → 7777777 2 digits → 1xxxxxxx | e.g. simulation 10 → 10000000 (note: x → last digit of simulation)
Source detector distance (SDD)		1000 mm
Object detector distance (ODD)		50 mm
X-axes (source, object, detector alignment)		0 mm

Geometry

The simulation setup from the geometrical viewpoint consisted of a detector, phantom, cabinet and granite blocks (see Figure 37). The setup of the used detector is described in section 2.1.2.1. It is visualised in Figure 4 to Figure 6, and its specifications are presented in Table 2. The phantom (scatter grid) is described in section 2.1.2.2 and visualised in Figure 11 and Figure 12. For the cabinet, the "sandwich" version (see Table 4) was used as described in section 2.1.2.3. The granite blocks are described in section 2.1.2.4.

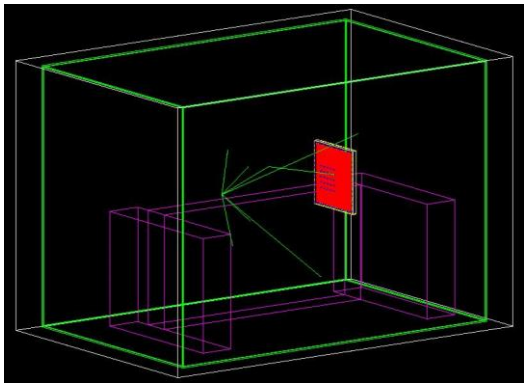

Figure 37: Configuration (p + cabs + gran) – simulation setup

The detector, source and phantom are placed at the world's centre (x-axes), which does not correspond with the actual placement in LuCi.

Source

For the X-ray source, the source spectrum with 160 kV acceleration voltage and 6.5 µm thick W target was used (see section 2.1.6). The full angle of the cone beam was set to 135°.

Physics processes

As a physics list, a predefined option called "emstandart_opt3" was used for the simulations. The production threshold was set to a cut length of 0.1 µm for all particles.

Data output

For the output, the actor macro file, which contains the DoseActor, was used. It produces a MetaImage, a combination of an mhd and a raw file, containing the energy deposition per pixel. The Image was set to a resolution of 864 by 864 pixels (see section 2.1.7.2). The resulting image files were further analysed with a Fiji macro (see section 2.2.8).

2.2.6 Configuration (pmx- + cab + gran)

This section details the system setup for the simulations with a phantom, a cabinet and the granite blocks. The results are documented in section 3.2.6. General information on the simulation setup is presented in Table 16.

Table 16: Configuration (pmx- + cabs + gran) – general information on setup

Parameter		Value
Primary particles	1st round	2e8
Engine seed	1st round	1 digit → xxxxxxx | e.g. simulation 7 → 7777777 2 digits → 1xxxxxxx | e.g. simulation 10 → 10000000 (note: x → last digit of simulation)
Source detector distance (SDD)		1000 mm
Object detector distance (ODD)		50 mm
X-axes (source, object, detector alignment)		-190 mm

Geometry

The simulation setup from a geometrical viewpoint consisted of a detector, phantom, cabinet and granite blocks (see Figure 38). The setup of the used detector is described in section 2.1.2.1. It is visualised in Figure 4 to Figure 6, and its specifications are presented in Table 2. The phantom (scatter grid) is described in section 2.1.2.2 and visualised in Figure 11 and Figure 12. For the cabinet, the "sandwich" version (see Table 4) was used as described in section 2.1.2.3. The granite blocks are described in section 2.1.2.4.

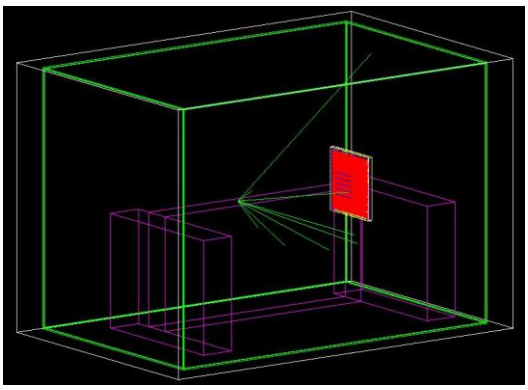

Figure 38: Configuration (pmx- + cabs + gran) – simulation setup

The detector, source and phantom are translated -190 mm along the x-axes from the world's centre, which corresponds with the actual placement in LuCi.

Source

For the X-ray source, the source spectrum with 160 kV acceleration voltage and 6.5 µm thick W target was used (see section 2.1.6). The full angle of the cone beam was set to 135°.

Physics processes

As a physics list, a predefined option called "emstandart_opt3" was used for the simulations. The production threshold was set to a cut length of 0.1 µm for all particles.

Data output

For the output, the actor macro file, which contains the DoseActor, was used. It produces a MetaImage, a combination of an mhd and a raw file, containing the energy deposition per pixel. The Image was set to a resolution of 864 by 864 pixels (see section 2.1.7.2). The resulting image files were further analysed with a Fiji macro (see section 2.2.8).

2.2.7 Configuration (pmx- + cab + gran + dh + oh)

This section describes the system setup for the simulations with a phantom, a cabinet, the granite blocks, the detector holder and the object holder. The results are documented in section 3.2.7. General information on the simulation setup is presented in Table 17.

Table 17: Configuration (pmx- + cab + gran + dh + oh) – general information on setup

Parameter		**Value**
Primary particles	1st round	2e8
Engine seed	1st round	1 digit → xxxxxxx | e.g. simulation 7 → 7777777 2 digits → 1xxxxxxx | e.g. simulation 10 → 10000000 (note: x → last digit of simulation)
Source detector distance (SDD)		1000 mm
Object detector distance (ODD)		50 mm
X-axes (source, object, detector alignment)		-190 mm

Geometry

The simulation setup can be seen in Figure 39. The setup of the used detector is described in section 2.1.2.1. It is visualised in Figure 4 to Figure 6, and its specifications are presented in Table 2. The phantom (scatter grid) is described in section 2.1.2.2 and visualised in Figure 11 and Figure 12. For the cabinet, the 1-layer version (see Table 4) was used as described in section 2.1.2.3. The granite blocks are described in section 2.1.2.4, the detector holder in section 2.1.2.5 and the object holder in section 2.1.2.6.

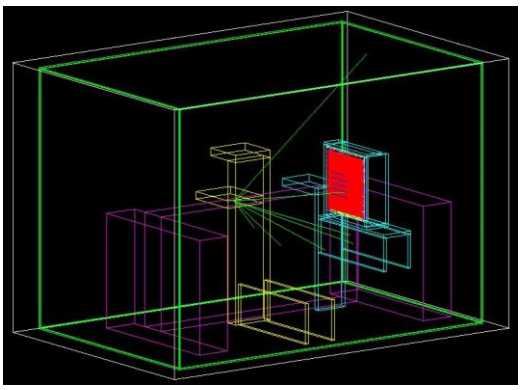

Figure 39: Configuration (pmx- + cab + gran + dh + oh) – simulation setup

The detector, source and phantom are translated -190 mm along the x-axes from the world's centre, which corresponds with the actual placement in LuCi.

Source

For the X-ray source, the source spectrum with 160 kV acceleration voltage and 6.5 µm thick W target was used (see section 2.1.6). The full angle of the cone beam was set to 135°.

Physics processes

As a physics list, the option "emstandart_opt3" was used for the simulations. The production threshold was set to a cut length of 0.1 µm for all particles.

Data output

For the output, the actor macro file was used, which contains the DoseActor. It produces a MetaImage, a combination of an mhd and a raw file, containing the energy deposition per pixel. The Image was set to a resolution of 864 by 864 pixels (see section 2.1.7.2). The resulting image files were further analysed with a Fiji macro (see section 2.2.8).

2.2.8 Image and data analysis

Each simulation produces a MetaImage, a combination of an mhd and a raw file. These output files were visualised and further analysed with a program called Fiji. Figure 40 shows such an image file, in which the energy deposition is represented by the grey value of each pixel. The numbering of the individual cylinders, which was used in the further analysis, is shown in the same figure.

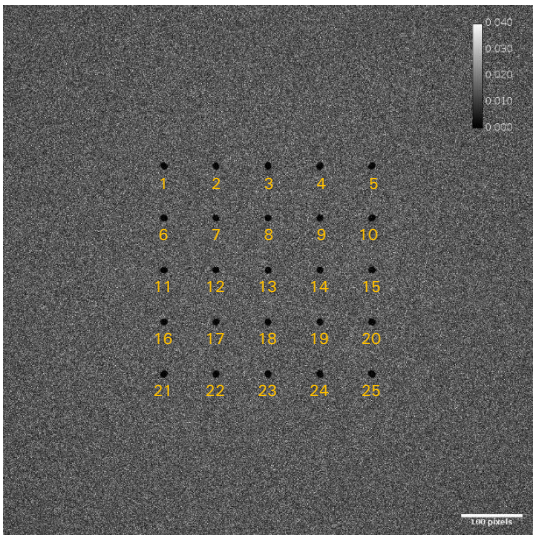

Figure 40: CT-Image energy deposition – 1 simulation

For the analysis of the 16 simulations of each configuration, two methods were used for the calculation of the mean and standard deviation (SD) of the scattered radiation for each of the 25 cylinders. Each method is further described in the following sections.

2.2.8.1 2-datasets

The first method is based on splitting the 16 simulation/images into two sets of eight, from which the mean and SD was calculated. The first eight and the second eight images were combined into one image each (see Figure 41) by adding them to a stack and summing up the grey values of the individual pixels.

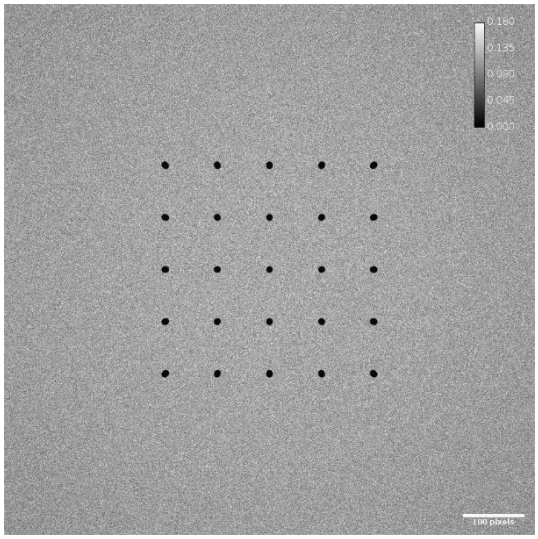

Figure 41: CT-Image energy deposition – 8 simulations summed up

The scattered radiation (energy deposition) of all 25 cylinders (see Figure 41) was calculated with a Fiji macro-file (see Appendix B.3.1.1). The macro-file measures the grey value of the shadow for each of the 25 cylinders as well as of the whole detector area. For each measurement, the four values – area, mean, min and max – are saved in a csv-file. The energy deposition is then calculated by multiplying the area with the mean value.

To calculate the scattered radiation for each cylinder, the sum of the energy deposition of all cylinders was first subtracted from the energy deposition of the whole detector area, and then the energy deposition of the individual cylinder was divided by the before, through subtraction, acquired energy deposition. All the measured and calculated values (area, mean, energy deposition, scattered radiation) were then saved into a text file.

For further analysis, Microsoft Excel was used. The calculated scattered radiation of both sets of eight simulations was used to calculate the mean and SD of the scattered radiation for all 25 cylinders individually. Additionally, the mean and SD of the means of the 25 individual cylinders was calculated to facilitate comparison of the scattered radiation between the individual configurations. For the overall mean and SD, a homogeneous distribution of the scattered radiation over all cylinders is assumed.

2.2.8.2 Bootstrapping

In order to reduce the SD from the results acquired with the method described in section 2.2.8.1, a statistical method called bootstrapping was used.

First, the scattered radiation (energy deposition) of all 25 cylinders was calculated for all 16 simulations/images with an extended Fiji macro-file (see Appendix B.3.1.2) based on that described in section 2.2.8.1. The extended macro-file analyses the 16 simulations automatically and saves the values for scattered radiation of each cylinder in all 16 simulations in a .csv-file for further analysis (applying bootstrapping).

The bootstrapping was run for each configuration/dataset with 10000 subsamples of size 16 from the original sample data with replacement. The bootstrapping of the data from the .csv-file mentioned above was applied by the supervisor and industry partner of this thesis.

The mean and SD of all individual 25 cylinders for all configurations was then further analysed in Microsoft Excel by calculating the mean and SD of the means of the individual cylinders before being visualised graphically.

3 Results

This section documents all the results obtained during the thesis, divided into sections. The first sections focus on the results produced during the development of a simulation setup in GATE for the simulation of scattered radiation. Later sections focus on the simulated scattered radiation results for different configurations and their comparison. The estimated scattered radiation results were further compared with the estimated results.

3.1 General simulation setup

The following sections present the interim results acquired during the development of a simulation setup in GATE, allowing, to a certain extent, a representation of LuCi and the measurement of scattered radiation within the simulated system.

3.1.1 Physics processes

Figure 42 depicts the comparison of the energy deposition spectrum for the predefined and self-defined physics list. For the methodology, see section 2.1.9.

Overall, the energy deposition acquired with the self-defined physics list (turquoise) is higher than emstandard_opt3 (purple). Additionally, the results for the self-defined physics list (turquoise) show a prominent edge at around 33 keV.

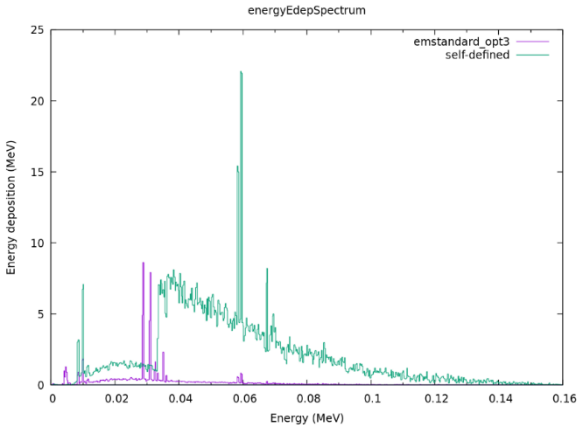

Figure 42: Energy deposition spectrum – predefined (emstandard_opt3) vs self-defined physics list

When comparing the self-defined and predefined physics lists, the first only includes processes for gamma particles and electrons. It was assumed that the difference of energy deposition could be caused by other particles, possibly ions.

Hence, the energy deposition spectrum of both physics lists was further analysed by performing additional simulations with four particle filters (no filter, gamma filter, electron filter, ion filter) in place. The results, as shown in Figure 43 and Figure 44, show that for both physics lists no energy is deposited by ions (orange) (double-checked in histogram txt-files). Therefore, it can be concluded that the precluded processes for ions in the self-defined physics list are not the cause of the difference in energy deposition spectrum (see Figure 42).
Additionally, comparison of the results for electron filter and gamma filter, as shown in Figure 43 and Figure 44, demonstrates that the energy deposition of electrons for the predefined physics list is slightly larger for the lower energy range, up to about 30 keV. The energy deposition by gamma particles for the self-defined physics list is larger over the whole spectrum. The effect is smaller for energies up to about 33 keV and significantly larger after that point, with a declining difference to the predefined physics list for continuously larger energies.

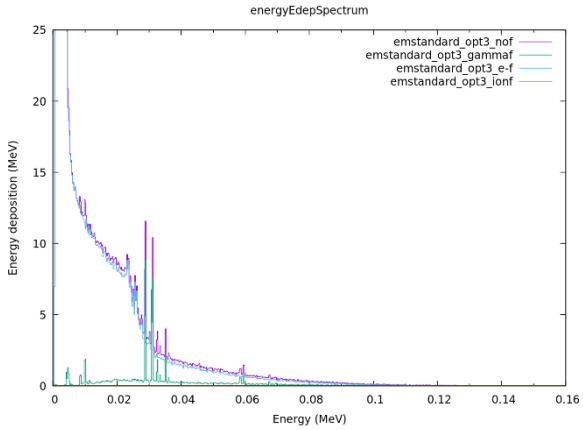

Figure 43: Energy deposition spectrum – predefined (emstandard_opt3) physics list (filter)

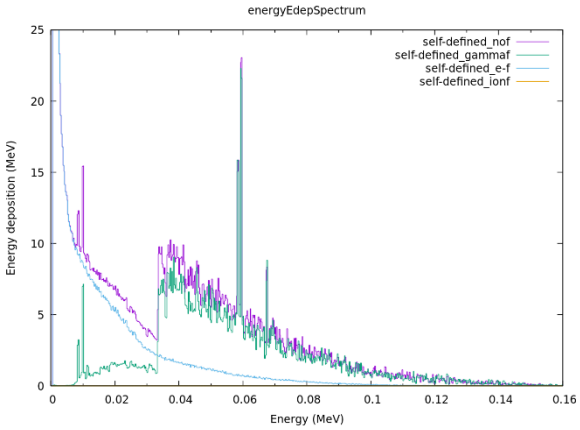

Figure 44: Energy deposition spectrum – self-defined physics list (filter)

In conclusion, the difference between the two physics list is caused by differences in the definition of the electron and gamma processes. As a reference point for further investigations into the definition of the gamma processes, the prominent edge at about 33 keV might be an indication because at this energy there is also a K-Edge of the CsI scintillator material (Berger et al., 2010). Generally, an exact replication of the emstandard_opt3 of GEANT4 in GATE is problematic because of the different naming and lack of settings in GATE.

3.1.2 Production threshold

Figure 45 to Figure 48 depict the comparison of the energy deposition spectrum for different cut lengths. For the methodology, see section 2.1.10.

Figure 45 and Figure 46 show the resulting energy deposition by changing the cut length only for gamma particles for a step multiplication of a factor 10 from 0.1 µm to 1 mm. The results show an increase of the energy deposition over the whole spectrum for an increasing cut length. For the 1 mm cut length (yellow), in particular, a high increase in energy deposition for photon energies over about 33 keV (prominent edge) is noticeable.

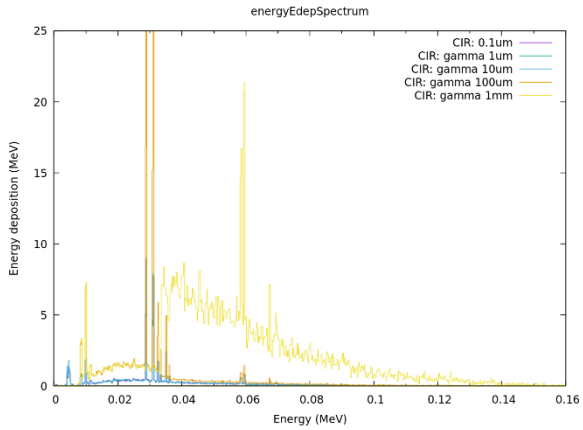

Figure 45: Energy deposition spectrum – gamma CutInRegion 0.1, 1, 10, 100, 1000 µm (25 MeV)

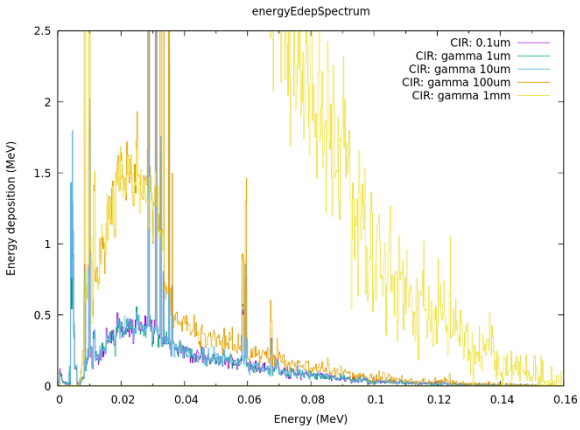

Figure 46: Energy deposition spectrum – gamma CutInRegion 0.1, 1, 10, 100, 1000 µm (2.5 MeV)

Figure 47 and Figure 48 demonstrate the resulting energy deposition by changing the cut length only for electrons for a step multiplication of a factor 10 from 0.1 µm to 1 mm. The results show an increase of the energy deposition over the whole spectrum for an increasing cut length.

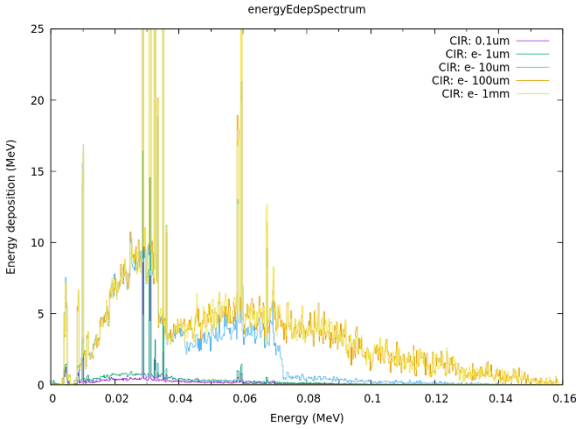

Figure 47: Energy deposition spectrum – electron CutInRegion 0.1, 1, 10, 100, 1000 µm (25 MeV)

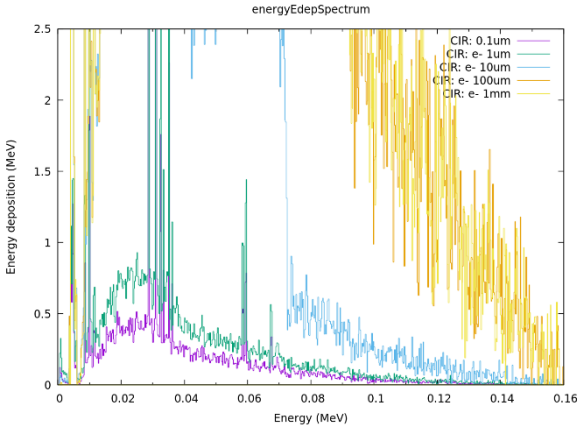

Figure 48: Energy deposition spectrum – electron CutInRegion 0.1, 1, 10, 100, 1000 µm (2.5 MeV)

Comparison of the results for the change in cut length for gamma particles with those obtained for electrons shows that the electrons' reaction on energy deposition is earlier, by a stepwise increase of the cut length, than for gamma particles. This is due to GATE's internal conversion of a cut length into an energy limit, depending on the particle type and material.

The production threshold essentially defines that all particles which travel further than the defined cut length are tracked further, and that the energy is deposited for each interaction within the material. For particles traveling a shorter distance than the defined cut length, the energy of the secondary particles is directly deposited instead of generating those secondary particles and tracking them. This leads to the conclusion that for a cut length longer than 1 mm (potentially also shorter), the energy of secondary particles generated in the 1-mm-thick scintillator material (energy deposition measurement) is deposited within it even though they might leave the detector.

3.2 Scattered radiation (simulated)

The following sections contain the results of the different configurations (see section 2.2) for the scattered radiation simulations. The final section gives an overview and comparison of all the different configurations. The results were obtained as described in section 2.2.8. For the raw data of the image analysis, see Appendix B.4.3 (configuration subfolder), and for further data processing, see Appendix B.3.2.

3.2.1 Configuration (p)

As described in section 2.2.8, two methods were implemented for the image analysis. With the first method, "2-datasets", the mean and SD of the scattered radiation for each individual cylinder was calculated (see Figure 49) from two sets of eight simulations each. The second method was to use bootstrapping for the calculation of the mean and SD of the individual cylinders (see Figure 50).

Table 18 gives an overview of the simulations with 1e8 and 2e8 primary particles as well as the two methods for the analysis. For 1e8 primary particles and the 2-datasets method, a mean of 3.90±0.48% of scattered radiation was calculated from the means of the individual cylinders. For the bootstrapping method, the result of the mean and SD over all cylinder means is similar, with a value of 3.90±0.47%. The range of the mean of the individual cylinders (2.95% to 5.47%) is the same for both methods of analysis. The change of the SD range is noticeable. The 2-datasets method's SD ranges from 0.00% to 1.35% over all cylinders. The bootstrapping method shows a significant reduction of the SD range (0.23% to 0.43%) as well as of the maximal value.
To enhance the results, it was decided to improve the raw data by increasing (doubling) the primary particles to 2e8. In comparison to the range of the means for 1e8 primary particles, the range was reduced for both methods (3.10% to 4.84%). In addition, the SD range for both methods was reduced, or at least the maximal SD was, with a result of 0.01% to 0.71% for the 2-dataset method and 0.15% to 0.41% for bootstrapping. In conclusion, for the configuration containing only the phantom, the result for the scattered radiation over all cylinders was 3.95±0.33% for the 2-dataset method and 3.96±0.33% for bootstrapping.

Table 18: Configuration (p) – scattered radiation overview

25 Cylinders			**Mean (%)**	**SD (%)**	**Min (%)**	**Max (%)**
1e8	2-datasets	Mean	3.90	0.48	2.95	5.47
		SD	-	-	0.00	1.35
	Bootstrapping	Mean	3.90	0.47	2.95	5.47
		SD	-	-	0.23	0.43
2e8	2-datasets	Mean	3.95	0.33	3.10	4.84
		SD	-	-	0.01	0.71
	Bootstrapping	Mean	3.96	0.33	3.10	4.84
		SD	-	-	0.15	0.41

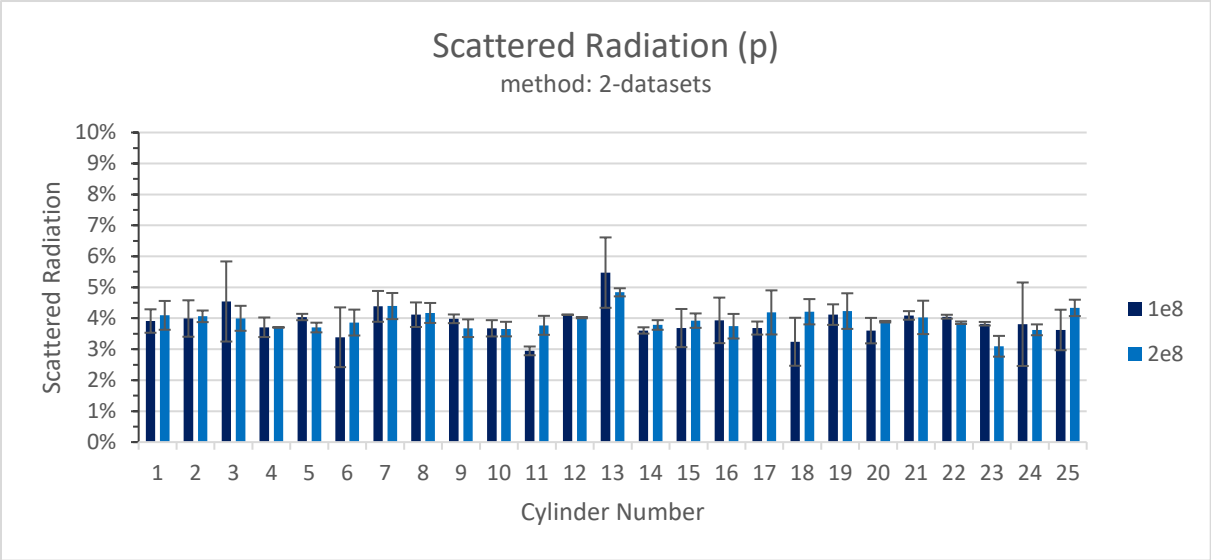

Figure 49: Configuration (p) – scattered radiation (2-datasets)

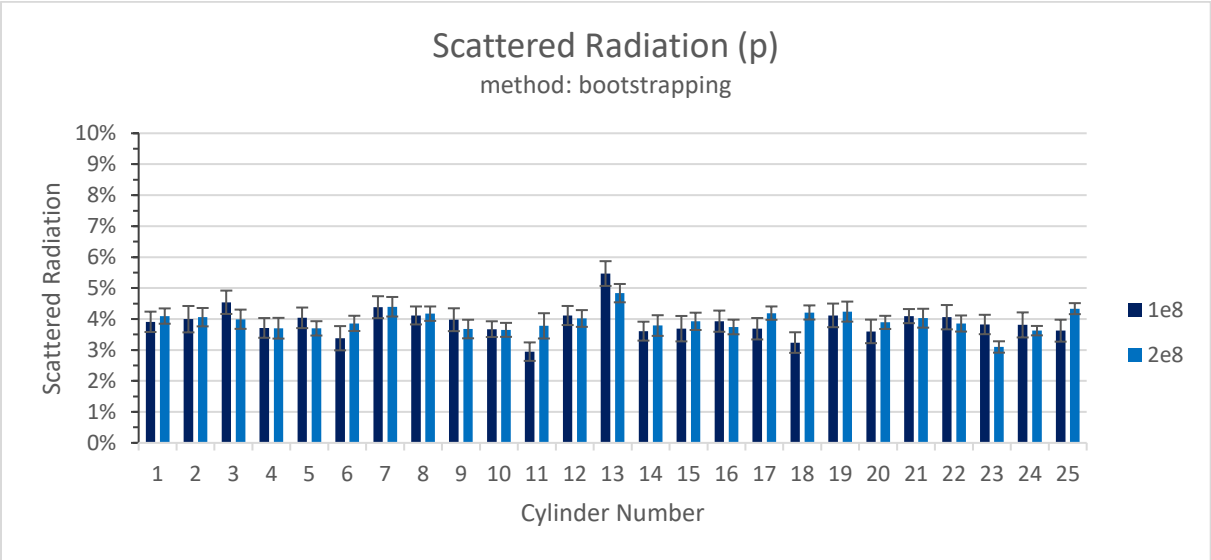

Figure 50: Configuration (p) – scattered radiation (bootstrapping)

3.2.2 Configuration (p + cab)

As described in section 2.2.8, two methods were used for the image analysis. Figure 51 depicts the results of the 2-datasets method while those of the bootstrapping are shown in Figure 52.

Table 19 gives an overview of the simulations with 1e8 and 2e8 primary particles as well as the two methods used for the analysis. For 1e8 primary particles and the 2-datasets method, a scattered radiation mean value of 4.44±0.50% was calculated. For the bootstrapping method, the result of the mean and SD overall cylinder means is similar, with a value of 4.44±0.49% for the scattered radiation. The ranges of the mean of the individual cylinders are similar, ranging from 3.18% to 5.36% for the 2-datasets method and from 3.18% to 5.35% for bootstrapping. The change of the SD range for both methods is noticeable. The 2-datasets method's SD ranges from 0.06% to 0.97% over all cylinders. The bootstrapping method shows a significant reduction of the SD range (0.23% to 0.50%) as well as of the maximal value.
As with the simulations including only the phantom, attempts were made to improve the raw data by doubling the primary particles to 2e8. In comparison to the range of the means for 1e8 primary particles, it was reduced for both methods, ranging from 3.80% to 6.04% for the 2-dataset method and from 3.81% to 6.05% for bootstrapping. In addition, the SD range for both methods was reduced or, at least, the maximal SD resulted in a range of 0.02% to 0.71% for the 2-dataset method and 0.18% to 0.35% for bootstrapping. For the configuration with the phantom and cabinet (1-layer), the scattered radiation result over all cylinders for both methods was 4.52±0.50%.

Table 19: Configuration (p + cab) – scattered radiation overview

25 Cylinders			Mean (%)	SD (%)	Min (%)	Max (%)
1e8	2-datasets	Mean	4.44	0.50	3.18	5.36
		SD	-	-	0.06	0.97
	Bootstrapping	Mean	4.44	0.49	3.18	5.35
		SD	-	-	0.23	0.50
2e8	2-datasets	Mean	4.52	0.50	3.80	6.04
		SD	-	-	0.02	0.71
	Bootstrapping	Mean	4.52	0.50	3.81	6.05
		SD	-	-	0.18	0.35

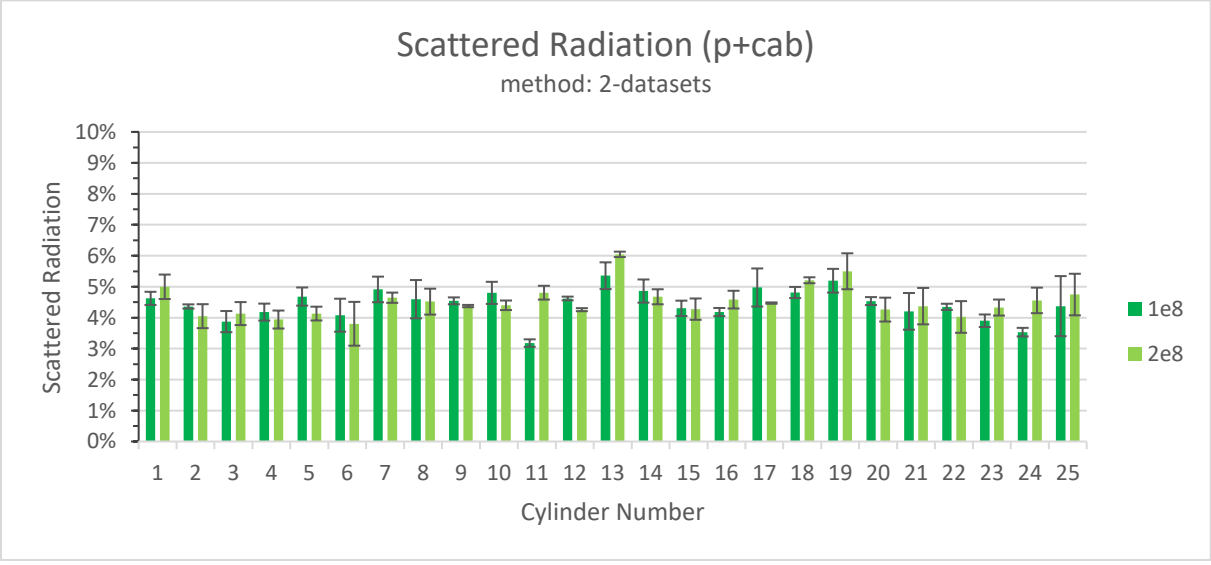

Figure 51: Configuration (p + cab) – scattered radiation (2-datasets)

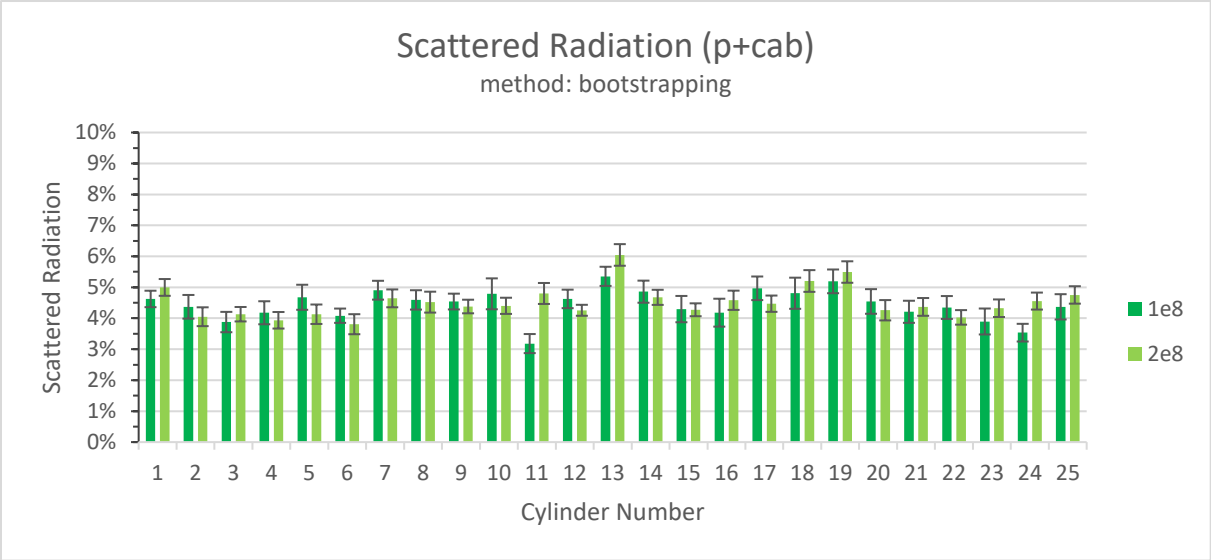

Figure 52: Configuration (p + cab) – scattered radiation (bootstrapping)

3.2.3 Configuration (p + gran)

Figure 53 and Figure 54 show the results for the two different methods (2-datasets and bootstrapping) described in section 2.2.8 which were used for image analysis.

Table 20 gives an overview of the simulations with 1e8 and 2e8 primary particles as well as the two methods used for the analysis. For 1e8 primary particles and both methods, the same scattered radiation mean value of 5.85±0.69% was calculated. The ranges of the mean of the individual cylinders are similar, ranging from 4.81% to 7.21% for the 2-datasets method and from 4.81% to 7.20% for bootstrapping. The change of the SD range for both methods is noticeable. The 2-datasets method's SD ranges from 0.02% to 1.70% over all cylinders. The bootstrapping method significantly reduces the SD range (0.32% to 0.59%) as well as the maximal value. In comparison to the range of the means for 1e8 primary particles, that for 2e8 (5.26% to 6.83%) was reduced for both methods. In addition, the SD range for both methods was reduced or, at least, the maximal SD was, with a result of 0.01% to 0.95% for the 2-dataset method and 0.19% to 0.40% for bootstrapping. The scattered radiation result for the phantom and granite blocks configuration for both methods over all cylinders was 5.85±0.44%.

Table 20: Configuration (p + gran) – scattered radiation overview

25 Cylinders			**Mean (%)**	**SD (%)**	**Min (%)**	**Max (%)**
1e8	2-datasets	Mean	5.85	0.69	4.81	7.21
		SD	-	-	0.02	1.70
	Bootstrapping	Mean	5.85	0.69	4.81	7.20
		SD	-	-	0.32	0.59
2e8	2-datasets	Mean	5.85	0.44	5.26	6.83
		SD	-	-	0.01	0.95
	Bootstrapping	Mean	5.85	0.44	5.26	6.83
		SD	-	-	0.19	0.40

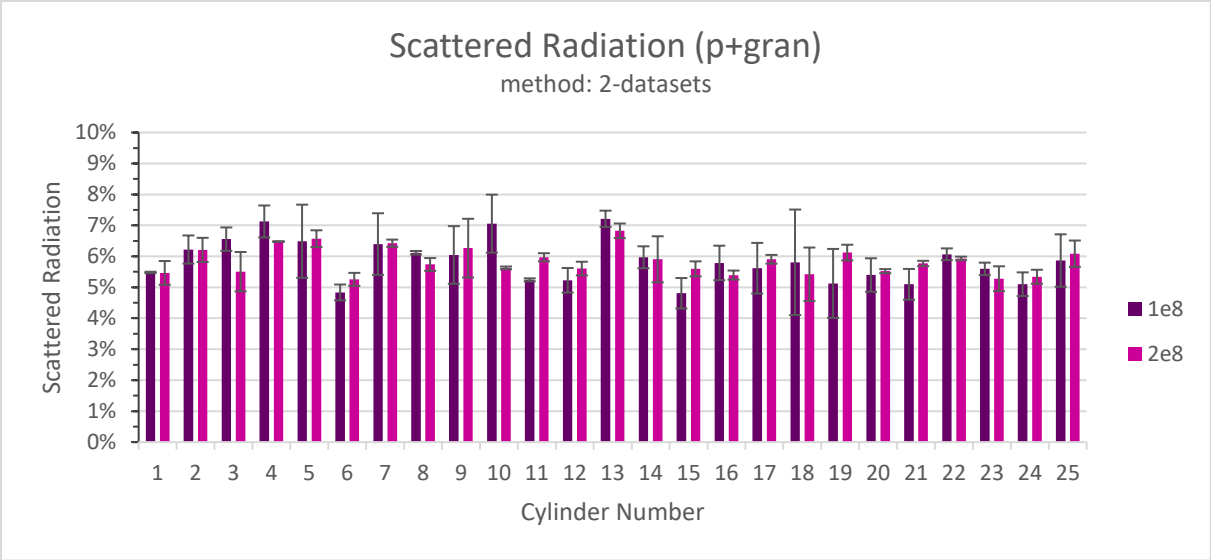

Figure 53: Configuration (p + gran) – scattered radiation (2-datasets)

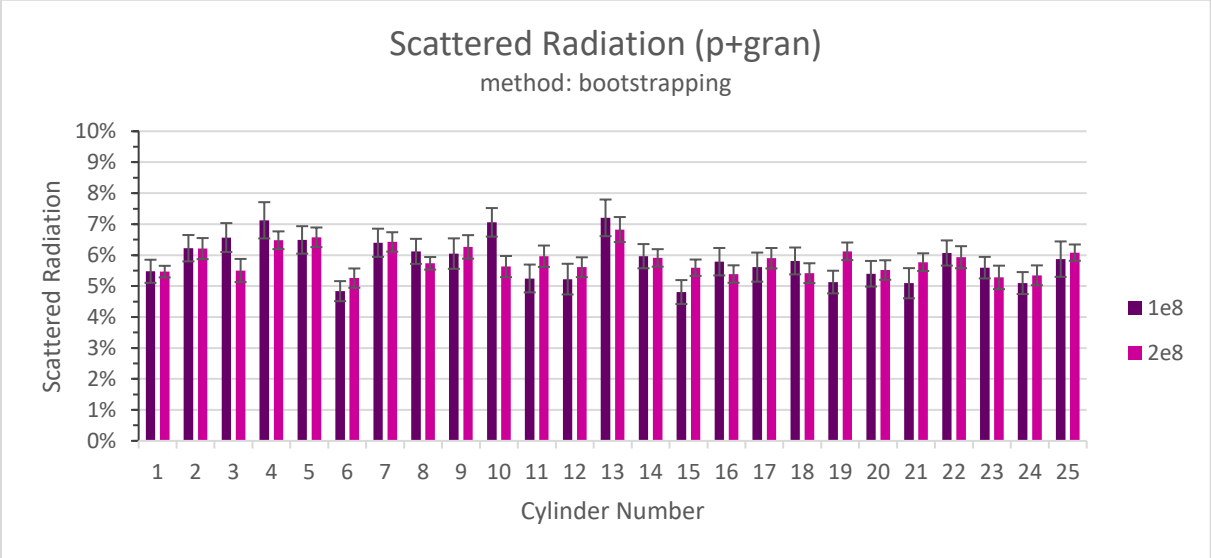

Figure 54: Configuration (p + gran) – scattered radiation (bootstrapping)

3.2.4 Configuration (p + cab + gran)

Section 2.2.8 details the two methods used for the image analysis. Figure 55 shows the results for the 2-datasets method, and Figure 56 shows those for the bootstrapping method.

An overview of the simulations with 1e8 and 2e8 primary particles, as well as the two methods for the analysis, is given in Table 21. For 1e8 primary particles and both methods, the same mean value for the scattered radiation (6.17±0.41%) was calculated. The range (5.34% to 6.91%) of the mean of the individual cylinders was the same for both methods. The change of the SD range for both methods was noticeable. The 2-datasets method's SD ranges from 0.02% to 1.41% over all cylinders. The bootstrapping method shows a significant reduction of the SD range (0.19% to 0.63%) as well as of the maximal value.
As with the other simulations, the primary particles were increased to 2e8. Comparing the range of the means to 1e8 primary particles, it was reduced for both methods, ranging from 5.27% to 6.85%. In addition, the SD range for both methods was reduced or, at least, the maximal SD was, with a result of 0.00% to 1.02% for the 2-dataset method and 0.21% to 0.46% for bootstrapping. In conclusion, the result for the scattered radiation over all cylinders for the configuration with the phantom, cabinet (1-layer) and granite blocks for both methods was 6.12±0.48%.

Table 21: Configuration (p + cab + gran) – scattered radiation overview

25 Cylinders			**Mean (%)**	**SD (%)**	**Min (%)**	**Max (%)**
1e8	2-datasets	Mean	6.17	0.41	5.34	6.91
		SD	-	-	0.02	1.41
	Bootstrapping	Mean	6.17	0.41	5.34	6.91
		SD	-	-	0.19	0.63
2e8	2-datasets	Mean	6.12	0.48	5.27	6.85
		SD	-	-	0.00	1.02
	Bootstrapping	Mean	6.12	0.48	5.27	6.85
		SD	-	-	0.21	0.46

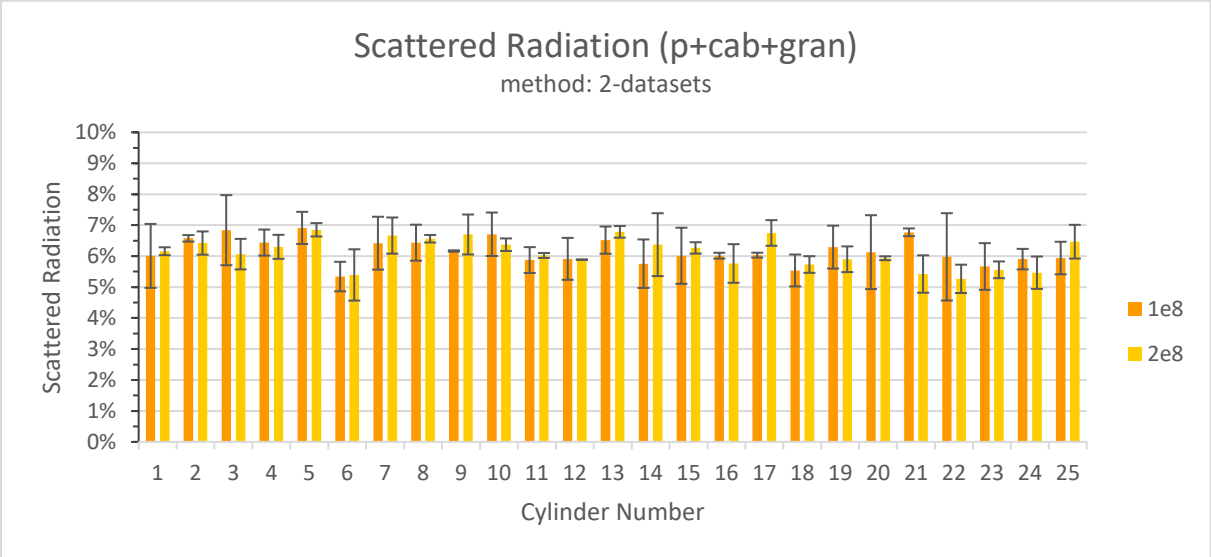

Figure 55: Configuration (p + cab + gran) – scattered radiation (2-datasets)

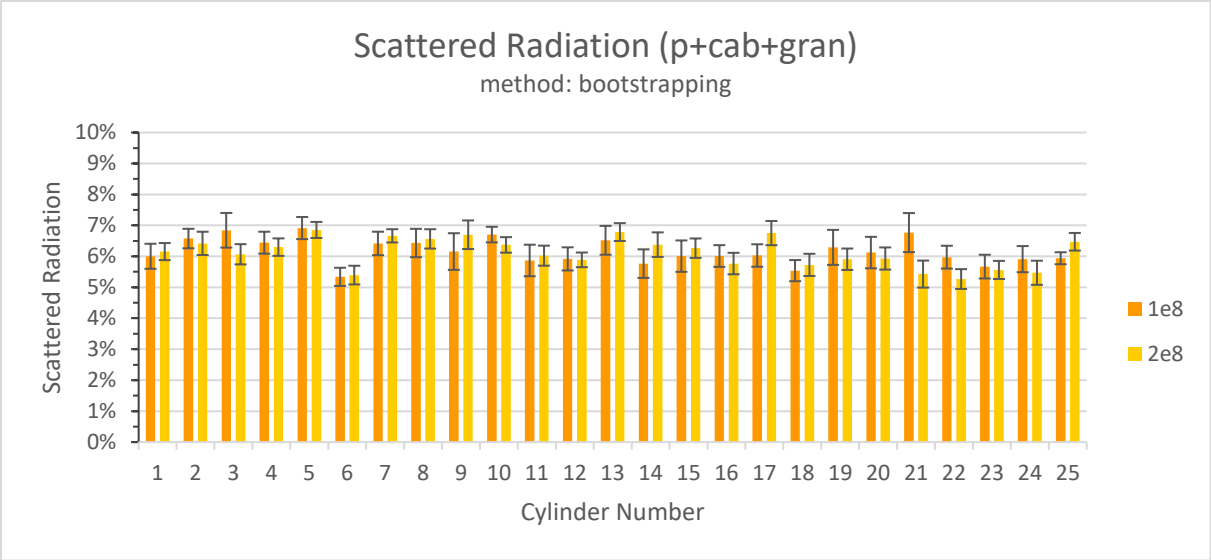

Figure 56: Configuration (p + cab + gran) – scattered radiation (bootstrapping)

3.2.5 Configuration (p + cabs + gran)

The results for the 2-datasets method are depicted in Figure 57, and Figure 58 shows those for the bootstrapping method. The methods are described in section 2.2.8.

When looking at the results of the configurations run with both 1e8 and 2e8 primary particles, it can be seen that, with the latter particle amount, the raw data is improved and the SD reduced. Therefore, the following simulation results were only calculated for 2e8 primary particles. Table 22 presents an overview of the results for both methods of analysis. The range of the mean of the individual cylinders is similar for both methods, ranging from 5.33% to 7.06% for the 2-datasets method and from 5.34% to 7.06% for bootstrapping. The change of the SD range for both methods is noticeable. The 2-datasets method's SD ranges from 0.00% to 1.30% over all cylinders. The bootstrapping method shows a significant reduction of the SD range (0.24% to 0.40%) as well as of the maximal value. The scattered radiation for the phantom, cabinet (sandwich) and granite blocks configuration over all cylinders was 6.04±0.43% for both methods.

Table 22: Configuration (p + cabs + gran) – scattered radiation overview

25 Cylinders			**Mean (%)**	**SD (%)**	**Min (%)**	**Max (%)**
2e8	2-datasets	Mean	6.04	0.43	5.33	7.06
		SD	-	-	0.00	1.30
	Bootstrapping	Mean	6.04	0.43	5.34	7.06
		SD	-	-	0.24	0.40

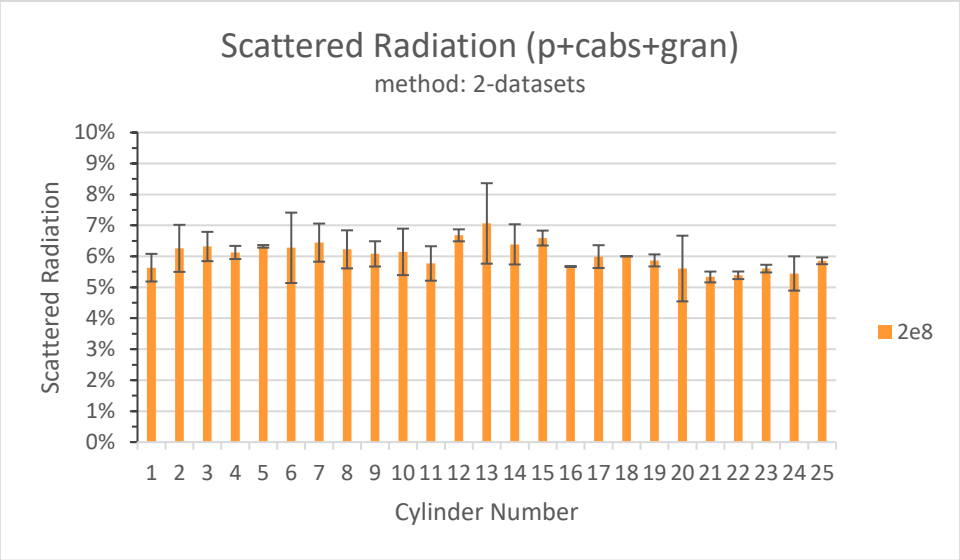

Figure 57: Configuration (p + cabs + gran) – scattered radiation (2-datasets)

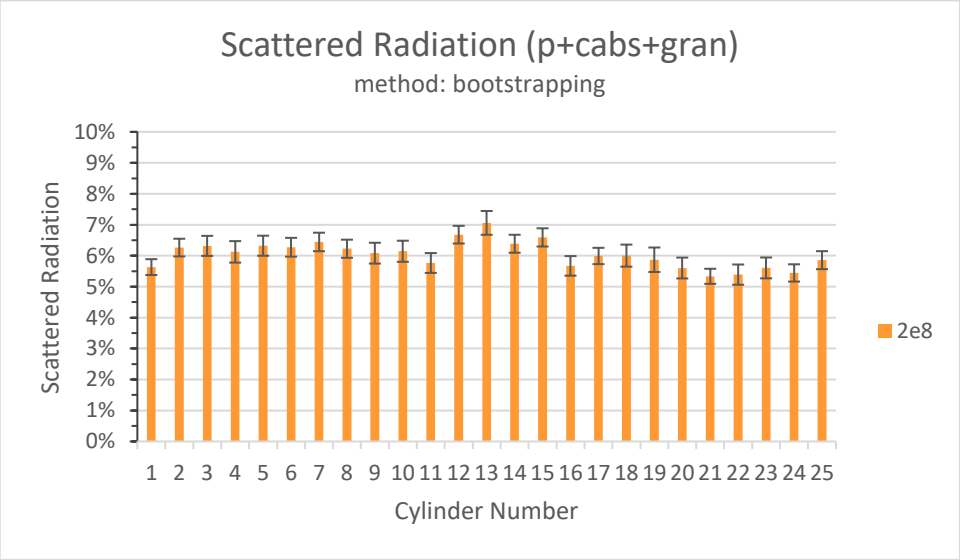

Figure 58: Configuration (p + cabs + gran) – scattered radiation (bootstrapping)

3.2.6 Configuration (pmx- + cab + gran)

Figure 59 and Figure 60 show the results for the two methods of image analysis used (see section 2.2.8) for the configuration including the phantom (actual placement), cabinet (1-layer) and granite blocks.

From the results of the configurations run with 1e8 and 2e8 primary particles, it was deduced that further simulation results were needed only for 2e8 primary particles, improving the raw data and, therefore, already reducing the SD of the raw data. Table 23 presents an overview of the results for both methods of analysis with 2e8 primary particles. The range of the mean of the individual cylinders is 4.89% to 6.57% for both methods. The change of the SD range for both methods is noticeable. The 2-datasets method's SD ranges from 0.03% to 1.34% over all cylinders. The bootstrapping method shows a significant reduction of the SD range (0.17% to 0.45%) as well as of the maximal value. In conclusion, the result for the scattered radiation over all cylinders for this configuration for both methods was 5.65±0.38%.

Table 23: Configuration (pmx- + cab + gran) – scattered radiation overview

25 Cylinders			**Mean (%)**	**SD (%)**	**Min (%)**	**Max (%)**
2e8	2-datasets	Mean	5.65	0.38	4.89	6.57
		SD	-	-	0.03	1.34
	Bootstrapping	Mean	5.65	0.38	4.89	6.57
		SD	-	-	0.17	0.45

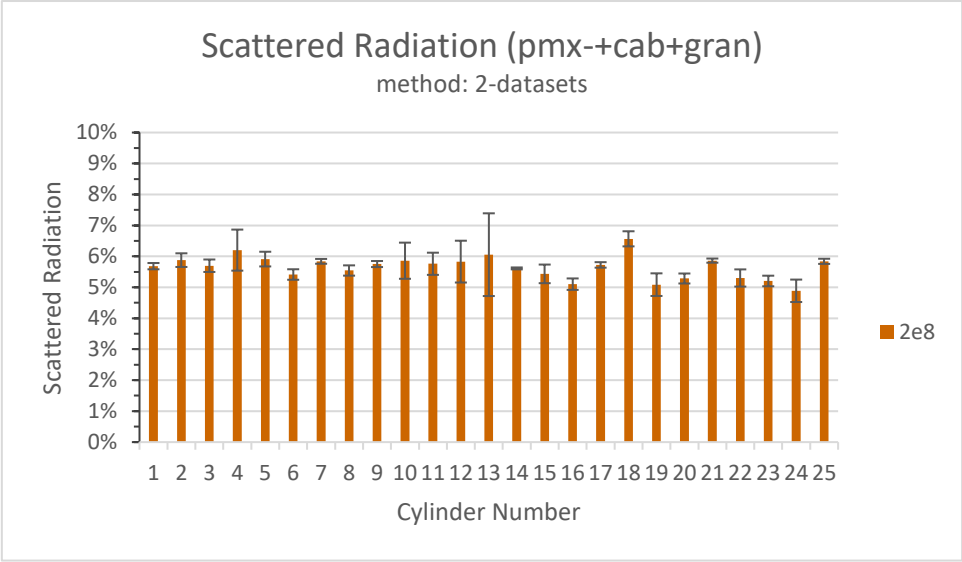

Figure 59: Configuration (pmx- + cab + gran) – scattered radiation (2-datasets)

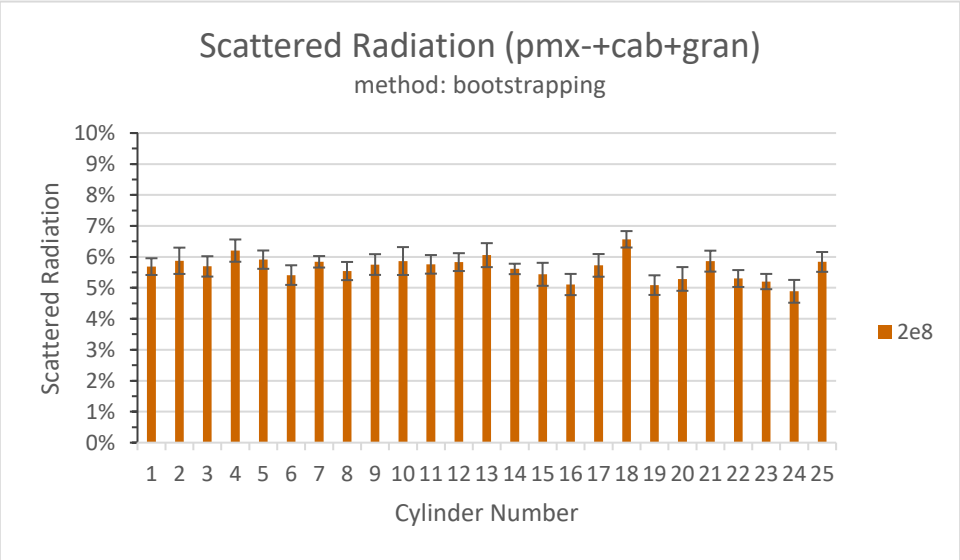

Figure 60: Configuration (pmx- + cab + gran) – scattered radiation (bootstrapping)

3.2.7 Configuration (pmx- + cab + gran + dh + oh)

For the final configuration the same image, 2-datasets and bootstrapping methods of analysis were implemented (see section 2.2.8). The results can be seen in Figure 61 and Figure 62, respectively.

Table 24 gives an overview of the results for both methods of analysis with 2e8 primary particles. The range of the mean of the individual cylinders is 5.61% to 6.89% for both methods. The change in the SD range is noticeable. The 2-datasets method's SD ranges from 0.01% to 1.07% over all cylinders. The bootstrapping method shows a significant reduction of the SD range (0.23% to 0.47%) as well as of the maximal value. In conclusion, the result for the scattered radiation over all cylinders for the configuration with the phantom (actual placement), cabinet (1-layer), granite blocks, detector holder and object holder for both methods was 6.25±0.40%.

Table 24: Configuration (pmx- + cab + gran +dh +oh) – scattered radiation overview

25 Cylinders			**Mean (%)**	**SD (%)**	**Min (%)**	**Max (%)**
2e8	2-datasets	Mean	6.25	0.40	5.61	6.89
		SD	-	-	0.01	1.07
	Bootstrapping	Mean	6.25	0.40	5.61	6.89
		SD	-	-	0.23	0.47

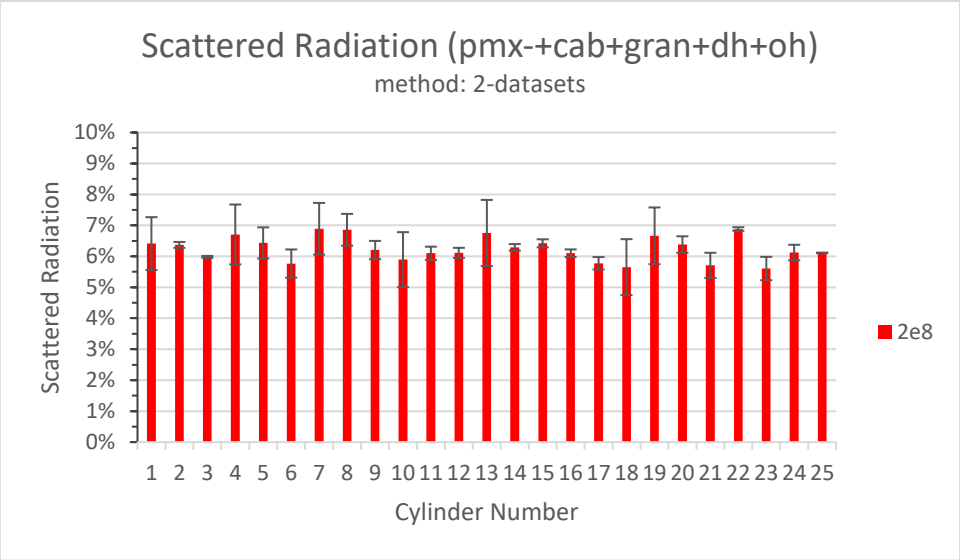

Figure 61: Configuration (pmx- + cab + gran + do + oh) – scattered radiation (2-datasets)

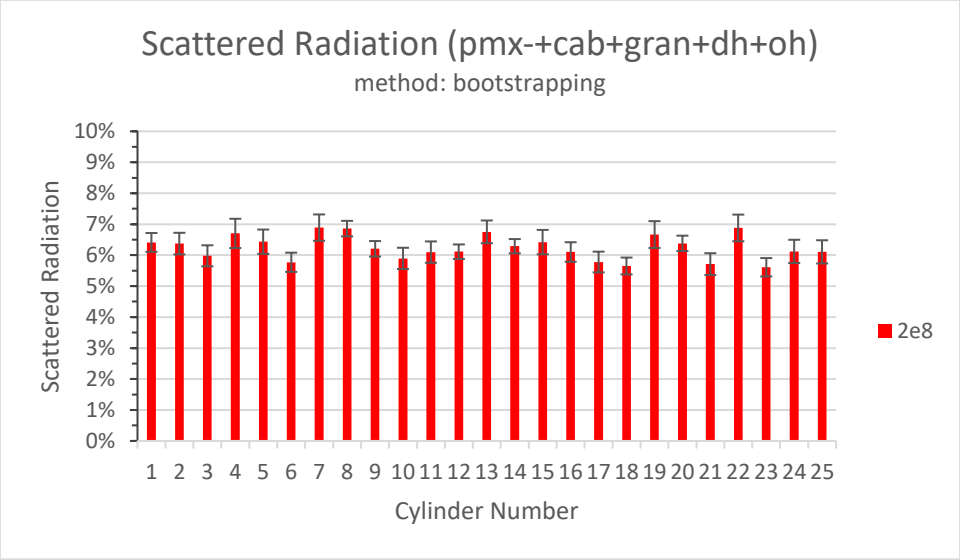

Figure 62: Configuration (pmx- + cab + gran + do + oh) – scattered radiation (bootstrapping)

3.2.8 Configuration Comparison

For a simplified comparison of the configurations, the mean and SD of the 25 cylinders means was calculated per configuration. Table 25 and Figure 63 show only the results for the simulations with 2e8 primary particles and bootstrapping as method of analysis. The results for the 2-datasets method show only a small difference of about 0.01% for certain values.

The granite blocks make the most noticeable contribution to the scattered radiation, compared to a setup with only a phantom, and show a difference of 1.89% for the scattered radiation. The detector holder's and object holder's (6.25±0.40%) contribution to the scattered radiation is smaller, resulting in a difference of 0.60% to the setup with a phantom, cabinet (1-layer) and granite blocks (5.65±0.38%). The smallest contribution to the scattered radiation comes from the cabinet (4.52±0.50%), with a difference of 0.56% to the setup with only a phantom (3.96±0.33%).

Some of the simulations were carried out with a different setup to that of LuCi. On the one hand, these are the cabinet versions cab (1-layer), where cabs (sandwich) was the most accurate, and, on the other, the placement of the source, phantom and detector alignment p (centred) and pmx- (moved in x-direction) later being the actual position.
Comparison of the results of the configuration phantom, cabinet and granite blocks shows that the calculated scattered radiation of 6.12±0.48% for the 1-layer cabinet version differs 0.08% from the "sandwich" version, with 6.04±0.0.43%. Additionally, comparison of the phantom, cabinet and granite blocks configurations reveals a difference of 0.47% in scattered radiation between the centred position (6.12±0.48%) and the actual position (5.65±0.38%). In conclusion, a reduction in scattered radiation of 0.08% for rerunning "cab" simulations with the more accurate cabinet (cabs) and a 0.47% reduction for rerunning "p" simulations with the actual position (pmx-) is expected. Except for the simulation with only a phantom because the only difference of moving the source, phantom and detector alignment, is that there is more air on one side than the other. This is negligible, considering scattering by air itself is negligible.

Table 25: Configuration comparison – scattered radiation overview (bootstrapping)

All Cylinders	**2e8**			
	Mean[1] (%)	**SD[2] (%)**	**Mean[1]-SD[2] (%)**	**Mean[1] + SD[2] (%)**
p	3.96	0.33	3.63	4.29
p + cab	4.52	0.50	4.02	5.02
p + gran	5.85	0.44	5.41	6.29
p + cab + gran	6.12	0.48	5.64	6.60
p + cabs + gran	6.04	0.43	5.61	6.47
pmx- + cab + gran	5.65	0.38	5.27	6.03
pmx- + cab + gran + dh + oh	6.25	0.40	5.85	6.65
Note: [1] mean of all means (25 cylinder) [2] SD of all means (25 cylinder)				

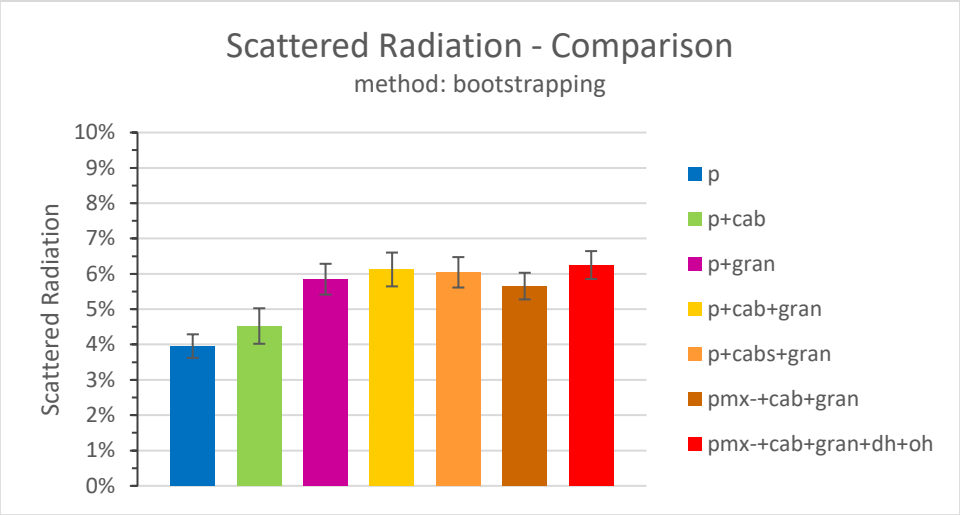

Figure 63: Configuration comparison – scattered radiation (bootstrapping)

3.3 Scattered radiation (experimental)

Experimental measurements of the scattered radiation within LuCi were carried out at LUASA by the team of CC TES, simultaneously with the simulations of the scattered radiation. General information on the simulation setup is presented in Table 26.

The results for the scattered radiation for the scatter grid are shown in Figure 64. The scattered radiation of the cylinders individually ranges from 12.0% to 13.1%. The mean over all cylinders is 12.57%, with a SD of ±0.34%.

Table 26: LuCi – General information on setup

Parameter		**Value**
Scatter grid	Diameter	5 mm
	Height	10 mm
	Spacing	40 mm (centre to centre)
	Material	Lead
Object detector distance (ODD)		50 mm

Figure 64: LuCi – scattered radiation

3.4 Scattered radiation (comparison)

Comparison of the results for the simulated approach (see section 3.2, especially section 3.2.7) and experimental approach (see section 3.3) reveals a significant difference in scattered radiation. The scattered radiation result for the simulation with a full setup (phantom, cabinet, granite blocks, detector holder, object holder) is 6.25%±0.40%, and for the experimental method it is 12.57±0.34%, which results in a difference of 6.32%.

4 Discussion

Plausibility of results

The simulated scattered radiation results differ significantly from the estimated results. To a certain extent, the reasons can be found in the differences between the simulation setup and the actual setup within LuCi. From a geometrical point of view, only those geometrical parts of the CT system which were assumed to be most prominent were introduced into the simulation setup. As a further factor, the simulated materials for the different parts are an approximation because of LuCi's lack of material specifications. Hence, it is not entirely clear whether the differences in scattered radiation can be explained only by the known setup differences or whether there might be additional causes leading to the different results for simulated and estimated scattered radiation.

Reflection on achievement of the aims

With the aim to conduct research into CT scanners and methods for the estimation and reduction of scattered radiation, a foundation for the further development of a simulation setup was established. The conclusion thereof was that GATE, a Monte Carlo simulation tool kit, is a suitable computer programme for the simulation of scattered radiation by rebuilding the actual setup of LuCi.

LuCi was only recreated to a certain extent within the simulation setup. A source spectrum, simulated with a mono-energy electron beam, was used as the source for the simulation. The individual components were measured by hand, leaving a certain margin for error, as there was no CAD model of LuCi available. Additionally, the materials of the individual parts were often based on approximations. Furthermore, the ratio of the self-defined materials, such as granite and steel, was based on the most common compositions. Another difficulty was rebuilding the detector, as there is only a limited amount of information on the individual components.

To acquire the scatter contribution of different parts, multiple simulations for different configurations were run. The additional aim – of taking measurements using different combinations of scattering effects – was not pursued further due to the unreliable results for the self-defined physics list in comparison to those of the predefined physics list emstandard_opt3. At the end of the thesis, the simulated scattered radiation for the scatter grid could be compared to the experimentally measured scattered radiation from LuCi itself.

Reflection on hypotheses

Research showed that Monte Carlo simulations (GATE) are a widely accepted method for the simulation of CT scans and therefore also for the simulation of scattered radiation.

According to the GATE documentation it is possible to simulate and calculate the contribution of specific physical effects to total amount of scattered radiation. However, the required definition of an own physics list did not lead to acceptable simulation results in comparison to the predefined physics list. Therefore, this aim could not be further pursued.

By averaging the results for the individual cylinders, the amount of simulated scattered radiation for the complete setup (phantom, detector, cabinet, granite blocks, detector holder and object holder) is 6.25±0.40%. These values are significantly smaller than the experimental measurement results of 8% scattering obtained before the start of this thesis. This difference is more pronounced in regard to the most recently obtained experimental measurements of 12.57±0.34% of scattered radiation.

5 Conclusion

The aim of this thesis was the development of a simulation setup for the estimation of scattered radiation, based on the CT system LuCi at LUASA. GATE, a Monte Carlo simulation tool kit, was used to achieve this objective because of its implementation in multiple studies and wide recognition by the scientific community.

The scattered radiation simulated for the full setup (phantom, cabinet, granite blocks, detector holder and object holder) is 6.25±0.40%. The biggest contributors to scattered radiation are the granite blocks, with a 1.89% difference to a setup with only a phantom. The detector holder's and object holder's contribution to the scattered radiation is 0.60%, and for the cabinet, a contribution of 0.56% was calculated. A reduction of these contributions is expected in the rerun of the simulations with the adjusted placement of the source, phantom and detector alignment as well as the switch to the cabinet "sandwich" version. The comparison of the simulated scattered radiation of this full setup (6.25±0.40%) with the most recently experimentally measured scattered radiation (12.57±0.34%) shows a significant difference of 6.32%.

Owing to the measured differences between the simulated and estimated scattered radiation, the simulation setup in GATE was only partly successful, as research shows that GATE is a viable simulation tool for such applications. Generally, the aim of simulating the scattered radiation by defining individual components was successful. The differences outlined above in scattered radiation show that further analysis into the simulation setup is needed. To a certain extent, the different results can be explained by known differences in geometrical representation as well as assumptions regarding the choice of material and material definition because of a lack of information. As soon as the CAD model of LuCi (currently in contact with manufacturer) is available, some uncertainties in the geometrical definition of the simulation setup can be remedied.

Further simulations for all configurations are needed for the newest simulation setup (sandwich cabinet, moved source phantom detector alignment). These are currently in progress. Additionally, simulations for future changes derived from the CAD model should be run to obtain more accurate results. Simulations with varying distances between phantom and detector, as well as source and detector, are needed in order to extract information on the impact of these changes on the simulated scattered radiation. To improve the simulation, the number of simulations per configuration as well as the number of primary particles should be increased for the reduction of uncertainties in the raw data (depending on computational power). An additional point to look into, as soon as the issues in geometrical representation are resolved, is the definition of an own physics list, in order to take measurements with different combinations of physical scattering effects.

List of figures

List of tables

List of references

Ay, M. R., & Zaidi, H. (2005). Development and validation of MCNP4C-based Monte Carlo simulator for fan- and cone-beam x-ray CT. *Physics in Medicine and Biology*, *50*(20), 4863–4885. https://doi.org/10.1088/0031-9155/50/20/009

Berger, M. J., Hubbell, J. H., Seltzer, S. M., Chang, J., Coursey, J. S., Sukumar, R., Zucker, D. S., & Olsen, K. (2010). *XCOM: Photon Cross Section Database (version 1.5)*. National Institute of Standards and Technology, Gaithersburg, MD. https://doi.org/10.18434/T48G6X

CERN Acceleration sciences. (2021). *GEANT4 A Simulation Toolkit*. https://geant4.web.cern.ch/

Chan, H. P., & Doi, K. (1983). The validity of Monte Carlo simulation in studies of scattered radiation in diagnostic radiology. *Physics in Medicine and Biology*, *28*(2), 109–129. https://doi.org/10.1088/0031-9155/28/2/001

Chantler, C. T. (1995). Theoretical Form Factor, Attenuation, and Scattering Tabulation for Z =1–92 from E =1–10 eV to E =0.4–1.0 MeV. *Journal of Physical and Chemical Reference Data*, *24*(1), 71–643. https://doi.org/10.1063/1.555974

Copley, D. C., Eberhard, J. W., & Mohr, G. A. (1994). Computed tomography part I: Introduction and industrial applications. *JOM*, *46*(1), 14–26. https://doi.org/10.1007/BF03222531

Hochschule Luzern. (2020). *Luci, ein Computertomograph für die Energieforschung*. https://www.hslu.ch/de-ch/hochschule-luzern/ueber-uns/medien/medienmitteilungen/2020/07/10/ein-computertomograph-fuer-die-energieforschung/

Inanc, F. (1999). Analysis of X-Ray and Gamma Ray Scattering Through Computational Experiments. *Journal of Nondestructive Evaluation*, *18*(2), 73–82. https://doi.org/10.1023/A:1022670305682

Jan, S., Benoit, D., Becheva, E., Carlier, T., Cassol, F., Descourt, P., Frisson, T., Grevillot, L., Guigues, L., Maigne, L., Morel, C., Perrot, Y., Rehfeld, N., Sarrut, D., Schaart, D. R., Stute, S., Pietrzyk, U., Visvikis, D., Zahra, N., & Buvat, I. (2011). GATE V6: a major enhancement of the GATE simulation platform enabling modelling of CT and radiotherapy. *Physics in Medicine and Biology*, *56*(4), 881–901. https://doi.org/10.1088/0031-9155/56/4/001

Kalender, W. (1981). Monte Carlo calculations of x-ray scatter data for diagnostic radiology. *Physics in Medicine and Biology*, *26*(5), 835–849. https://doi.org/10.1088/0031-9155/26/5/003

Kyriakou, Y., Riedel, T., & Kalender, W. A. (2006). Combining deterministic and Monte Carlo calculations for fast estimation of scatter intensities in CT. *Physics in Medicine and Biology*, *51*(18), 4567–4586. https://doi.org/10.1088/0031-9155/51/18/008

Miceli, A., Thierry, R., Bettuzzi, M., Flisch, A., Hofmann, J., Sennhauser, U., & Casali, F. (2007). Comparison of simulated and measured spectra of an industrial 450kV X-ray tube. *Nuclear Instruments and Methods in Physics Research Section A: Accelerators, Spectrometers, Detectors and Associated Equipment*, *580*(1), 123–126. https://doi.org/10.1016/j.nima.2007.05.025

Miceli, A., Thierry, R., Flisch, A., Sennhauser, U., Casali, F., & Simon, M. (2007). Monte Carlo simulations of a high-resolution X-ray CT system for industrial applications. *Nuclear Instruments and Methods in Physics Research Section A: Accelerators, Spectrometers, Detectors and Associated Equipment*, *583*(2), 313–323. https://doi.org/10.1016/j.nima.2007.09.012

OpenGATE Collaboration. (2021). *Welcome to GATE's documentation!* https://opengate.readthedocs.io/_/downloads/en/latest/pdf/

Schoerner, K. (2012). *Development of Methods for Scatter Artifact Correction in Industrial X-ray Cone-beam Computed Tomography* [Technical University of Munich]. https://mediatum.ub.tum.de/doc/1097730/document.pdf

Schuetz, P., Miceli, A., Jerjen, I., Flisch, A., Hofmann, J., Broennimann, R., & Sennhauser, U. (2013).

Reducing environmental scattering in industrial computed tomography by system redesign. *NDT & E International*, *58*, 36–42. https://doi.org/10.1016/j.ndteint.2013.04.005

Appendix

Table of Content

A. GATE macro-files

In the following sections are the individual macro-files for an exemplary simulation setup listed. In this case the macro files for the simulation described in section 2.2.7 were used.

A.1. Main

Filename: main_clu0comp90_sgPbmx-_cab_gran_dh_oh_std_module_c135full_1.mac

```
#=====================================================
# VERBOSITY
#=====================================================

/control/execute   mac/verbose/verbose.mac

#=====================================================
# VISUALISATION
#=====================================================

#/control/execute    mac/visu/visu.mac

#=====================================================
# GEOMETRY
#=====================================================

/control/execute    mac/geometry/world_2x2x3.mac
/control/execute    mac/geometry/detector/cluster0_comp90_1mm_mx-.mac
/control/execute    mac/geometry/phantom/scattergrid_5mm_Pb_mx-.mac
/control/execute    mac/geometry/cabinet/cabinet.mac
/control/execute    mac/geometry/granite/granite.mac
/control/execute    mac/geometry/detectorholder/detectorholder.mac
/control/execute    mac/geometry/objectholder/objectholder.mac

#=====================================================
# PHYSICS
#=====================================================

/control/execute    mac/physics/standard.mac

#=====================================================
# ACTOR
#=====================================================

/control/execute    mac/output/actor864_1.mac

#=====================================================
# INITIALISATION
#=====================================================

/gate/run/initialize

#=====================================================
# DIGITIZER
#=====================================================

/control/execute    mac/digitizer/digitizer.mac

#=====================================================
# SOURCE
#=====================================================

/control/execute    mac/source/160kV-65um_cone135_full90_mx-.mac

#=====================================================
# OUTPUT
#=====================================================

#/control/execute    mac/output/output.mac
#/gate/output/allowNoOutput

#=====================================================
# MAIN
#=====================================================

/gate/random/setEngineName MersenneTwister
/gate/random/setEngineSeed 1111111

/gate/application/setTotalNumberOfPrimaries 2e8
/gate/application/start
exit
```

A.1.1. Visualisation

Filename: visu.mac

```
#/vis/open OGL
#/vis/open OGLSX
#/vis/open OGLI
/vis/open OGLIQt

/vis/drawVolume
/vis/viewer/flush
/tracking/storeTrajectory            1
/vis/scene/add/trajectories
/vis/scene/endOfEventAction          accumulate

#/vis/scene/add/axes            0 0 0 1000 mm
#/vis/scene/add/text            10 0 0 cm  20 0 0   X
#/vis/scene/add/text            0 10 0 cm  20 0 0   Y
#/vis/scene/add/text            0 0 10 cm  20 0 0   Z
/vis/viewer/set/auxiliaryEdge true

#/vis/viewer/zoom 4
#/vis/viewer/panTo 300 0 mm
/vis/viewer/set/viewpointThetaPhi -90 0 deg
```

A.1.2. Verbosity

Filename: verbose.mac

```

/gate/verbose Physic    0
/gate/verbose Cuts      0
/gate/verbose SD        0
/gate/verbose Actions   0
/gate/verbose Actor     0
/gate/verbose Step      0
/gate/verbose Error     10
/gate/verbose Warning   10
/gate/verbose Output    0
/gate/verbose Beam      0
/gate/verbose Volume    0
/gate/verbose Image     0
/gate/verbose Geometry  0
/gate/verbose Core      0

/run/verbose 0
/event/verbose 0
/tracking/verbose 0
```

A.1.3. Geometry

Filename: world_2x2x3.mac

```
/gate/geometry/setMaterialDatabase  data/GateMaterials.db

#*************************************************************
#   WORLD           -->     Depth 0                          *
#*************************************************************
# WORLD
/gate/world/setMaterial                     Air
/gate/world/geometry/setXLength             2 m
/gate/world/geometry/setYLength             2 m
/gate/world/geometry/setZLength             3 m
/gate/world/vis/forceWireframe
/gate/world/vis/setColor                    white
```

A.1.3.1. Detector

Filename: cluster0_comp90_1mm_mx-.mac

```
#*********************************************************
#   CT-Scanner      -->     Depth 1                       *
#*********************************************************
# CT-SCANNER
/gate/world/daughters/name                  CTscanner
/gate/world/daughters/insert                box
/gate/CTscanner/placement/setTranslation    -190 40 636 mm #1000-1920/2
#1000(SDD)-380+0.5*thickness
/gate/CTscanner/geometry/setXLength         470 mm
/gate/CTscanner/geometry/setYLength         470 mm
/gate/CTscanner/geometry/setZLength         32 mm
/gate/CTscanner/setMaterial                 Air
/gate/CTscanner/vis/forceWireframe
/gate/CTscanner/vis/setColor                white


#*********************************************************
#   Housing         -->     Depth 1                       *
#*********************************************************
# CT-SCANNER  ---->  FRONTPANEL
/gate/CTscanner/daughters/name              frontpanel
/gate/CTscanner/daughters/insert            box
/gate/frontpanel/placement/setTranslation   0 0 -15.5 mm
/gate/frontpanel/geometry/setXLength        466 mm
/gate/frontpanel/geometry/setYLength        466 mm
/gate/frontpanel/geometry/setZLength        1 mm
/gate/frontpanel/setMaterial                Epoxy
/gate/frontpanel/vis/forceWireframe
/gate/frontpanel/vis/setColor               magenta

# CT-SCANNER  ---->  BACKPANEL
/gate/CTscanner/daughters/name              backpanel
/gate/CTscanner/daughters/insert            box
/gate/backpanel/placement/setTranslation    0 0 15 mm
/gate/backpanel/geometry/setXLength         466 mm
/gate/backpanel/geometry/setYLength         466 mm
/gate/backpanel/geometry/setZLength         2 mm
/gate/backpanel/setMaterial                 Aluminium
/gate/backpanel/vis/forceWireframe
/gate/backpanel/vis/setColor                yellow

# CT-SCANNER  ---->  RIGHTPANEL
/gate/CTscanner/daughters/name              r_panel
/gate/CTscanner/daughters/insert            box
/gate/r_panel/placement/setTranslation      -234 0 0 mm
/gate/r_panel/geometry/setXLength           2 mm
/gate/r_panel/geometry/setYLength           470 mm
/gate/r_panel/geometry/setZLength           32 mm
/gate/r_panel/setMaterial                   Aluminium
/gate/r_panel/vis/forceWireframe
/gate/r_panel/vis/setColor                  yellow

# CT-SCANNER  ---->  LEFTPANEL
/gate/CTscanner/daughters/name              l_panel
/gate/CTscanner/daughters/insert            box
/gate/l_panel/placement/setTranslation      234 0 0 mm
/gate/l_panel/geometry/setXLength           2 mm
/gate/l_panel/geometry/setYLength           470 mm
/gate/l_panel/geometry/setZLength           32 mm
/gate/l_panel/setMaterial                   Aluminium
/gate/l_panel/vis/forceWireframe
/gate/l_panel/vis/setColor                  yellow

# CT-SCANNER  ---->  TOPPANEL
/gate/CTscanner/daughters/name              t_panel
/gate/CTscanner/daughters/insert            box
/gate/t_panel/placement/setTranslation      0 234 0 mm
/gate/t_panel/geometry/setXLength           466 mm
/gate/t_panel/geometry/setYLength           2 mm
/gate/t_panel/geometry/setZLength           32 mm
/gate/t_panel/setMaterial                   Aluminium
/gate/t_panel/vis/forceWireframe
/gate/t_panel/vis/setColor                  yellow
```

```
73
74  # CT-SCANNER  ---->  BOTTOMPANEL
75  /gate/CTscanner/daughters/name              b_panel
76  /gate/CTscanner/daughters/insert            box
77  /gate/b_panel/placement/setTranslation      0 -234 0 mm
78  /gate/b_panel/geometry/setXLength           466 mm
79  /gate/b_panel/geometry/setYLength           2 mm
80  /gate/b_panel/geometry/setZLength           32 mm
81  /gate/b_panel/setMaterial                   Aluminium
82  /gate/b_panel/vis/forceWireframe
83  /gate/b_panel/vis/setColor                  yellow
84
85
86  #************************************************************
87  #   Photodetector   -->     Depth 1                         *
88  #************************************************************
89  # CT-SCANNER  ---->  PDETECTOR
90  /gate/CTscanner/daughters/name              pdetector
91  /gate/CTscanner/daughters/insert            box
92  /gate/pdetector/placement/setTranslation    0 0 0 mm
93  /gate/pdetector/geometry/setXLength         432 mm
94  /gate/pdetector/geometry/setYLength         432 mm
95  /gate/pdetector/geometry/setZLength         28 mm
96  /gate/pdetector/setMaterial                 Silicon
97  /gate/pdetector/vis/forceWireframe
98  /gate/pdetector/vis/setColor                blue
99
100 # CT-SCANNER  ---->  RIGHTPDETECTOR
101 /gate/CTscanner/daughters/name              r_pdetector
102 /gate/CTscanner/daughters/insert            box
103 /gate/r_pdetector/placement/setTranslation  -224.5 0 -0.5 mm
104 /gate/r_pdetector/geometry/setXLength       17 mm
105 /gate/r_pdetector/geometry/setYLength       466 mm
106 /gate/r_pdetector/geometry/setZLength       29 mm
107 /gate/r_pdetector/setMaterial               Silicon
108 /gate/r_pdetector/vis/forceWireframe
109 /gate/r_pdetector/vis/setColor              blue
110
111 # CT-SCANNER  ---->  LEFTPDETECTOR
112 /gate/CTscanner/daughters/name              l_pdetector
113 /gate/CTscanner/daughters/insert            box
114 /gate/l_pdetector/placement/setTranslation  224.5 0 -0.5 mm
115 /gate/l_pdetector/geometry/setXLength       17 mm
116 /gate/l_pdetector/geometry/setYLength       466 mm
117 /gate/l_pdetector/geometry/setZLength       29 mm
118 /gate/l_pdetector/setMaterial               Silicon
119 /gate/l_pdetector/vis/forceWireframe
120 /gate/l_pdetector/vis/setColor              blue
121
122 # CT-SCANNER  ---->  TOPPDETECTOR
123 /gate/CTscanner/daughters/name              t_pdetector
124 /gate/CTscanner/daughters/insert            box
125 /gate/t_pdetector/placement/setTranslation  0 224.5 -0.5 mm
126 /gate/t_pdetector/geometry/setXLength       432 mm
127 /gate/t_pdetector/geometry/setYLength       17 mm
128 /gate/t_pdetector/geometry/setZLength       29 mm
129 /gate/t_pdetector/setMaterial               Silicon
130 /gate/t_pdetector/vis/forceWireframe
131 /gate/t_pdetector/vis/setColor              blue
132
133 # CT-SCANNER  ---->  BOTTOMPDETECTOR
134 /gate/CTscanner/daughters/name              b_pdetector
135 /gate/CTscanner/daughters/insert            box
136 /gate/b_pdetector/placement/setTranslation  0 -224.5 -0.5 mm
137 /gate/b_pdetector/geometry/setXLength       432 mm
138 /gate/b_pdetector/geometry/setYLength       17 mm
139 /gate/b_pdetector/geometry/setZLength       29 mm
140 /gate/b_pdetector/setMaterial               Silicon
141 /gate/b_pdetector/vis/forceWireframe
142 /gate/b_pdetector/vis/setColor              blue
143
144
145 #************************************************************
146 #   Scintillator    -->     Depth 1                         *
147 #************************************************************
148 # CT-SCANNER  ---->  MODULE
149 /gate/CTscanner/daughters/name              module
150 /gate/CTscanner/daughters/insert            box
151 /gate/module/placement/setTranslation       0 0 -14.5 mm
152 /gate/module/geometry/setXLength            432 mm
153 /gate/module/geometry/setYLength            432 mm
154 /gate/module/geometry/setZLength            1 mm
155 /gate/module/setMaterial                    Air
156 /gate/module/vis/forceWireframe
157 /gate/module/vis/setColor                   white
```

```
158
159
160  #************************************************************
161  #   Cluster          -->     Depth 2                         *
162  #************************************************************
163  # MODULE  ----->  CLUSTER_0
164  /gate/module/daughters/name                cluster
165  /gate/module/daughters/insert              box
166  /gate/cluster/geometry/setXLength          432 mm
167  /gate/cluster/geometry/setYLength          432 mm
168  /gate/cluster/geometry/setZLength          1 mm
169  /gate/cluster/setMaterial                  Air
170  /gate/cluster/vis/forceWireframe
171  /gate/cluster/vis/setColor                 white
172
173
174  #************************************************************
175  #   Pixel            -->     Depth 3                         *
176  #************************************************************
177  # MODULE  ----->  CLUSTER_0  ----->  PIXEL_0
178  /gate/cluster/daughters/name               pixel
179  /gate/cluster/daughters/insert             box
180  /gate/pixel/geometry/setXLength            1 mm
181  /gate/pixel/geometry/setYLength            1 mm
182  /gate/pixel/geometry/setZLength            1 mm
183  /gate/pixel/setMaterial                    CsI
184  /gate/pixel/vis/setColor                   red
185
186  # REPEAT PIXEl_0
187  /gate/pixel/repeaters/insert               cubicArray
188  /gate/pixel/cubicArray/setRepeatNumberX    432
189  /gate/pixel/cubicArray/setRepeatNumberY    432
190  /gate/pixel/cubicArray/setRepeatNumberZ    1
191  /gate/pixel/cubicArray/setRepeatVector     1 1 0 mm
192  /gate/pixel/cubicArray/autoCenter          true
193
194  # ATTACH SYSTEM
195  /gate/systems/CTscanner/module/attach      module
196  /gate/systems/CTscanner/cluster_0/attach   cluster
197  /gate/systems/CTscanner/pixel_0/attach     pixel
198
199  # ATTACH LAYER
200  /gate/pixel/attachCrystalSD
```

A.1.3.2. Phantom

Filename: scattergrid_5mm_Pb_mx-.mac

```
1  /gate/world/daughters/name                 Cylinder
2  /gate/world/daughters/insert               cylinder
3  /gate/Cylinder/placement/setTranslation    -190 40 565 mm #1000-1920/2
   #636-16-50(ODD)-0.5*thickness
4  /gate/Cylinder/geometry/setRmax            2.5 mm
5  /gate/Cylinder/geometry/setHeight          10 mm
6  /gate/Cylinder/setMaterial                 Lead
7  /gate/Cylinder/vis/forceWireframe
8  /gate/Cylinder/vis/setColor                blue
9
10 /gate/Cylinder/repeaters/insert            cubicArray
11 /gate/Cylinder/cubicArray/setRepeatNumberX 5
12 /gate/Cylinder/cubicArray/setRepeatNumberY 5
13 /gate/Cylinder/cubicArray/setRepeatNumberZ 1
14 /gate/Cylinder/cubicArray/setRepeatVector  40 40 0 mm
15 /gate/Cylinder/cubicArray/autoCenter       true
16
17 /gate/Cylinder/attachPhantomSD
```

A.1.3.3. Cabinet

Filename: cabinet.mac

```
# Cabinet
/gate/world/daughters/name                  f_cabinet
/gate/world/daughters/insert                box
/gate/f_cabinet/placement/setTranslation    0 0 1355 mm #1350 + 0.5*thickness
/gate/f_cabinet/geometry/setXLength         1720 mm #1720 - thickness
/gate/f_cabinet/geometry/setYLength         1920 mm
/gate/f_cabinet/geometry/setZLength         10 mm
/gate/f_cabinet/setMaterial                 Lead
/gate/f_cabinet/vis/forceWireframe
/gate/f_cabinet/vis/setColor                green


/gate/world/daughters/name                  ba_cabinet
/gate/world/daughters/insert                box
/gate/ba_cabinet/placement/setTranslation   0 0 -1355 mm #-(1350 + 0.5*thickness)
/gate/ba_cabinet/geometry/setXLength        1720 mm #1720 - thickness
/gate/ba_cabinet/geometry/setYLength        1920 mm
/gate/ba_cabinet/geometry/setZLength        10 mm
/gate/ba_cabinet/setMaterial                Lead
/gate/ba_cabinet/vis/forceWireframe
/gate/ba_cabinet/vis/setColor               green


/gate/world/daughters/name                  r_cabinet
/gate/world/daughters/insert                box
/gate/r_cabinet/placement/setTranslation    865 0 0 mm #860 + 0.5*thickness
/gate/r_cabinet/geometry/setXLength         10 mm
/gate/r_cabinet/geometry/setYLength         1920 mm
/gate/r_cabinet/geometry/setZLength         2720 mm #2700 + 2*thickness
/gate/r_cabinet/setMaterial                 Lead
/gate/r_cabinet/vis/forceWireframe
/gate/r_cabinet/vis/setColor                green


/gate/world/daughters/name                  l_cabinet
/gate/world/daughters/insert                box
/gate/l_cabinet/placement/setTranslation    -865 0 0 mm #-(870 + 0.5*thickness)
/gate/l_cabinet/geometry/setXLength         10 mm
/gate/l_cabinet/geometry/setYLength         1920 mm
/gate/l_cabinet/geometry/setZLength         2720 mm #2700 + 2*thickness
/gate/l_cabinet/setMaterial                 Lead
/gate/l_cabinet/vis/forceWireframe
/gate/l_cabinet/vis/setColor                green


/gate/world/daughters/name                  t_cabinet
/gate/world/daughters/insert                box
/gate/t_cabinet/placement/setTranslation    0 965 0 mm #960 + 0.5*thickness
/gate/t_cabinet/geometry/setXLength         1740 mm #1720 + 2*thickness
/gate/t_cabinet/geometry/setYLength         10 mm
/gate/t_cabinet/geometry/setZLength         2720 mm #2700 + 2*thickness
/gate/t_cabinet/setMaterial                 Lead
/gate/t_cabinet/vis/forceWireframe
/gate/t_cabinet/vis/setColor                green


/gate/world/daughters/name                  bo_cabinet
/gate/world/daughters/insert                box
/gate/bo_cabinet/placement/setTranslation   0 -965 0 mm #-(960 + 0.5*thickness)
/gate/bo_cabinet/geometry/setXLength        1740 mm #1720 + 2*thickness
/gate/bo_cabinet/geometry/setYLength        10 mm
/gate/bo_cabinet/geometry/setZLength        2720 mm #2700 + 2*thickness
/gate/bo_cabinet/setMaterial                Lead
/gate/bo_cabinet/vis/forceWireframe
/gate/bo_cabinet/vis/setColor               green
```

A.1.3.4. Granite

Filename: granite.mac

```
# Granite
/gate/world/daughters/name                  f_granite
/gate/world/daughters/insert                box
/gate/f_granite/placement/setTranslation    -5 -535 1160 mm #-(860-(1150/2+280))
#-(960-850+850/2) #1350-65-0.5*thickness
/gate/f_granite/geometry/setXLength         1150 mm
/gate/f_granite/geometry/setYLength         850 mm
/gate/f_granite/geometry/setZLength         250 mm
/gate/f_granite/setMaterial                 Granite
/gate/f_granite/vis/forceWireframe
/gate/f_granite/vis/setColor                green


/gate/world/daughters/name                  ba_granite
/gate/world/daughters/insert                box
/gate/ba_granite/placement/setTranslation   -5 -535 -845 mm #-(860-(1150/2+280))
#-(960-850+850/2) #-(1350-380-0.5*thickness)
/gate/ba_granite/geometry/setXLength        1150 mm
/gate/ba_granite/geometry/setYLength        850 mm
/gate/ba_granite/geometry/setZLength        250 mm
/gate/ba_granite/setMaterial                Granite
/gate/ba_granite/vis/forceWireframe
/gate/ba_granite/vis/setColor               green


/gate/world/daughters/name                  l_granite
/gate/world/daughters/insert                box
/gate/l_granite/placement/setTranslation    340 -535 157.5 mm #860-420-0.5*thickness
#-(960-850+850/2) #1350-380-250-1150/2
/gate/l_granite/geometry/setXLength         200 mm
/gate/l_granite/geometry/setYLength         850 mm
/gate/l_granite/geometry/setZLength         1755 mm #2700-380-2*250-65
/gate/l_granite/setMaterial                 Granite
/gate/l_granite/vis/forceWireframe
/gate/l_granite/vis/setColor                green
```

A.1.3.5. Detector holder

Filename: detectorholder.mac

```
# Detectorholder
/gate/world/daughters/name                  dh
/gate/world/daughters/insert                box
/gate/dh/placement/setTranslation           -37.5 -327.5 740 mm
/gate/dh/geometry/setXLength                1255 mm
/gate/dh/geometry/setYLength                1265 mm
/gate/dh/geometry/setZLength                240 mm
/gate/dh/setMaterial                        Air
/gate/dh/vis/forceWireframe
/gate/dh/vis/setColor                       white
/gate/dh/vis/setVisible                     false

/gate/dh/daughters/name                     dh1
/gate/dh/daughters/insert                   box
/gate/dh1/placement/setTranslation          427.5 245 0 mm
/gate/dh1/geometry/setXLength               400 mm
/gate/dh1/geometry/setYLength               55 mm
/gate/dh1/geometry/setZLength               240 mm
/gate/dh1/setMaterial                       Aluminium
/gate/dh1/vis/forceWireframe
/gate/dh1/vis/setColor                      cyan

/gate/dh/daughters/name                     dh2
/gate/dh/daughters/insert                   box
/gate/dh2/placement/setTranslation          205 -180 0 mm
/gate/dh2/geometry/setXLength               45 mm
/gate/dh2/geometry/setYLength               905 mm
/gate/dh2/geometry/setZLength               240 mm
/gate/dh2/setMaterial                       Aluminium
/gate/dh2/vis/forceWireframe
/gate/dh2/vis/setColor                      cyan

/gate/dh/daughters/name                     dh3
/gate/dh/daughters/insert                   box
/gate/dh3/placement/setTranslation          -222.5 60 0 mm
/gate/dh3/geometry/setXLength               810 mm
/gate/dh3/geometry/setYLength               25 mm
/gate/dh3/geometry/setZLength               240 mm
/gate/dh3/setMaterial                       Aluminium
/gate/dh3/vis/forceWireframe
/gate/dh3/vis/setColor                      cyan
```

```
42
43  /gate/dh/daughters/name                     dh4
44  /gate/dh/daughters/insert                   box
45  /gate/dh4/placement/setTranslation          -222.5 -77.5 107.5 mm
46  /gate/dh4/geometry/setXLength               810 mm
47  /gate/dh4/geometry/setYLength               250 mm
48  /gate/dh4/geometry/setZLength               25 mm
49  /gate/dh4/setMaterial                       Aluminium
50  /gate/dh4/vis/forceWireframe
51  /gate/dh4/vis/setColor                      cyan
52
53  /gate/dh/daughters/name                     dh5
54  /gate/dh/daughters/insert                   box
55  /gate/dh5/placement/setTranslation          -222.5 -77.5 -107.5 mm
56  /gate/dh5/geometry/setXLength               810 mm
57  /gate/dh5/geometry/setYLength               250 mm
58  /gate/dh5/geometry/setZLength               25 mm
59  /gate/dh5/setMaterial                       Aluminium
60  /gate/dh5/vis/forceWireframe
61  /gate/dh5/vis/setColor                      cyan
62
63  #Detectorcasing
64  /gate/dh/daughters/name                     dc
65  /gate/dh/daughters/insert                   box
66  /gate/dc/placement/setTranslation           -152.5 352.5 -25 mm
67  /gate/dc/geometry/setXLength                530 mm
68  /gate/dc/geometry/setYLength                560 mm
69  /gate/dc/geometry/setZLength                190 mm
70  /gate/dc/setMaterial                        Air
71  /gate/dc/vis/forceWireframe
72  /gate/dc/vis/setColor                       white
73  /gate/dc/vis/setVisible                     false
74
75  /gate/dc/daughters/name                     dc1
76  /gate/dc/daughters/insert                   box
77  /gate/dc1/placement/setTranslation          0 -270 0 mm
78  /gate/dc1/geometry/setXLength               530 mm
79  /gate/dc1/geometry/setYLength               20 mm
80  /gate/dc1/geometry/setZLength               190 mm
81  /gate/dc1/setMaterial                       Aluminium
82  /gate/dc1/vis/forceWireframe
83  /gate/dc1/vis/setColor                      cyan
84
85  /gate/dc/daughters/name                     dc2
86  /gate/dc/daughters/insert                   box
87  /gate/dc2/placement/setTranslation          0 270 -30 mm
88  /gate/dc2/geometry/setXLength               530 mm
89  /gate/dc2/geometry/setYLength               20 mm
90  /gate/dc2/geometry/setZLength               130 mm
91  /gate/dc2/setMaterial                       Aluminium
92  /gate/dc2/vis/forceWireframe
93  /gate/dc2/vis/setColor                      cyan
94
95  /gate/dc/daughters/name                     dc3
96  /gate/dc/daughters/insert                   box
97  /gate/dc3/placement/setTranslation          250 0 0 mm
98  /gate/dc3/geometry/setXLength               30 mm
99  /gate/dc3/geometry/setYLength               520 mm
100 /gate/dc3/geometry/setZLength               190 mm
101 /gate/dc3/setMaterial                       Aluminium
102 /gate/dc3/vis/forceWireframe
103 /gate/dc3/vis/setColor                      cyan
104
105 /gate/dc/daughters/name                     dc4
106 /gate/dc/daughters/insert                   box
107 /gate/dc4/placement/setTranslation          -250 0 0 mm
108 /gate/dc4/geometry/setXLength               30 mm
109 /gate/dc4/geometry/setYLength               520 mm
110 /gate/dc4/geometry/setZLength               190 mm
111 /gate/dc4/setMaterial                       Aluminium
112 /gate/dc4/vis/forceWireframe
113 /gate/dc4/vis/setColor                      cyan
```

A.1.3.6. Object holder

Filename: objectholder.mac

```
# Objectholder
/gate/world/daughters/name                  oh
/gate/world/daughters/insert                box
/gate/oh/placement/setTranslation           -70 -330 0 mm
/gate/oh/geometry/setXLength                1320 mm
/gate/oh/geometry/setYLength                1260 mm
/gate/oh/geometry/setZLength                310 mm
/gate/oh/setMaterial                        Air
/gate/oh/vis/forceWireframe
/gate/oh/vis/setColor                       white
/gate/oh/vis/setVisible                     false

/gate/oh/daughters/name                     oh1
/gate/oh/daughters/insert                   box
/gate/oh1/placement/setTranslation          460 247.5 0 mm
/gate/oh1/geometry/setXLength               400 mm
/gate/oh1/geometry/setYLength               55 mm
/gate/oh1/geometry/setZLength               310 mm
/gate/oh1/setMaterial                       Aluminium
/gate/oh1/vis/forceWireframe
/gate/oh1/vis/setColor                      yellow

/gate/oh/daughters/name                     oh2
/gate/oh/daughters/insert                   box
/gate/oh2/placement/setTranslation          215 -27.5 0 mm
/gate/oh2/geometry/setXLength               90 mm
/gate/oh2/geometry/setYLength               1205 mm
/gate/oh2/geometry/setZLength               310 mm
/gate/oh2/setMaterial                       Aluminium
/gate/oh2/vis/forceWireframe
/gate/oh2/vis/setColor                      yellow

/gate/oh/daughters/name                     oh3
/gate/oh/daughters/insert                   box
/gate/oh3/placement/setTranslation          325 602.5 0 mm
/gate/oh3/geometry/setXLength               310 mm
/gate/oh3/geometry/setYLength               55 mm
/gate/oh3/geometry/setZLength               310 mm
/gate/oh3/setMaterial                       Aluminium
/gate/oh3/vis/forceWireframe
/gate/oh3/vis/setColor                      yellow

/gate/oh/daughters/name                     oh4
/gate/oh/daughters/insert                   box
/gate/oh4/placement/setTranslation          -245 -480 117.5 mm
/gate/oh4/geometry/setXLength               830 mm
/gate/oh4/geometry/setYLength               300 mm
/gate/oh4/geometry/setZLength               25 mm
/gate/oh4/setMaterial                       Aluminium
/gate/oh4/vis/forceWireframe
/gate/oh4/vis/setColor                      yellow

/gate/oh/daughters/name                     oh5
/gate/oh/daughters/insert                   box
/gate/oh5/placement/setTranslation          -245 -480 -117.5 mm
/gate/oh5/geometry/setXLength               830 mm
/gate/oh5/geometry/setYLength               300 mm
/gate/oh5/geometry/setZLength               25 mm
/gate/oh5/setMaterial                       Aluminium
/gate/oh5/vis/forceWireframe
/gate/oh5/vis/setColor                      yellow
```

A.1.4. Physics processes

Filename: standard.mac

```
/gate/physics/addPhysicsList            emstandard_opt3

/gate/physics/Gamma/SetCutInRegion      world 0.1 um
/gate/physics/Electron/SetCutInRegion   world 0.1 um
/gate/physics/Positron/SetCutInRegion   world 0.1 um
/gate/physics/Proton/SetCutInRegion     world 0.1 um

/gate/physics/processList  Enabled
/gate/physics/print output/physics.txt
/gate/physics/displayCuts
```

A.1.5. Digitizer

Filename: digitizer.mac

```
/gate/digitizer/Singles/insert adder
/gate/digitizer/Singles/insert readout
/gate/digitizer/Singles/readout/setDepth 2
#/gate/digitizer/Singles/insert thresholder
#/gate/digitizer/Singles/thresholder/setThreshold 10 keV


# E N E R G Y B L U R R I N G
#/gate/digitizer/Singles/insert blurring
#/gate/digitizer/Singles/blurring/setResolution 0.19
#/gate/digitizer/Singles/blurring/setEnergyOfReference 511. keV
# E N E R G Y W I N D O W
#/gate/digitizer/Singles/insert thresholder
#/gate/digitizer/Singles/thresholder/setThreshold 350. keV
#/gate/digitizer/Singles/insert upholder
#/gate/digitizer/Singles/upholder/setUphold 650. keV
```

A.1.6. Source

Filename: 160kV-65um_cone135_full90_mx-.mac

```
/gate/source/addSource histogram            gps
/gate/source/histogram/gps/particle         gamma
/gate/source/histogram/gps/energytype       UserSpectrum
/gate/source/histogram/gps/setSpectrumFile
data/Energy-65um-W-Tube-160kV_energySpectrumFluenceTrack.txt

/gate/source/histogram/gps/ang/type         iso
/gate/source/histogram/gps/ang/mintheta     0 deg
/gate/source/histogram/gps/ang/maxtheta     67.5 deg #135°

/gate/source/histogram/gps/pos/type         Plane
/gate/source/histogram/gps/pos/shape        Circle
/gate/source/histogram/gps/pos/radius       5 um
/gate/source/histogram/gps/pos/centre       -190 40 -380 mm #1000-1920/2
#-(2700/2-970)
#/gate/source/histogram/gps/pos/rot1         1 0 0

/gate/source/histogram/visualize            0 yellow 5 cm
```

A.1.7. Data output

Filename: actor864_1.mac

```
#Stat
/gate/actor/addActor    SimulationStatisticActor        stat
/gate/actor/stat/addFilter                              particleFilter
/gate/actor/stat/particleFilter/addParticle             gamma
/gate/actor/stat/save                                   output/864/2e8/1/stats.txt

#Energy spectrum
/gate/actor/addActor    EnergySpectrumActor             EnergyActor
/gate/actor/EnergyActor/addFilter                       particleFilter
/gate/actor/EnergyActor/particleFilter/addParticle      gamma
/gate/actor/EnergyActor/attachTo                        module
/gate/actor/EnergyActor/saveAsText                      true
/gate/actor/EnergyActor/save
output/864/2e8/1/Energy_module.root
#/gate/actor/EnergyActor/normalizeToNbPrimaryEvents     true


/gate/actor/EnergyActor/energySpectrum/setEmin          0 eV
/gate/actor/EnergyActor/energySpectrum/setEmax          160 keV
/gate/actor/EnergyActor/energySpectrum/setNumberOfBins  640


/gate/actor/EnergyActor/enableNbPartSpectrum            true
/gate/actor/EnergyActor/enableFluenceTrackSpectrum      true


/gate/actor/EnergyActor/enableEdepSpectrum              true
/gate/actor/EnergyActor/enableEdepHisto                 false
/gate/actor/EnergyActor/enableEdepTimeHisto             false
/gate/actor/EnergyActor/enableEdepTrackHisto            false
/gate/actor/EnergyActor/enableElossHisto                true
/gate/actor/EnergyActor/energyLossHisto/setEmin         0 eV
/gate/actor/EnergyActor/energyLossHisto/setEmax         160 keV
/gate/actor/EnergyActor/energyLossHisto/setNumberOfBins 640


#Energy deposition
/gate/actor/addActor    DoseActor                       DoseActor
/gate/actor/DoseActor/addFilter                         particleFilter
/gate/actor/DoseActor/particleFilter/addParticle        gamma
/gate/actor/DoseActor/attachTo                          module
#/gate/actor/DoseActor/saveAsText                       true
#/gate/actor/DoseActor/save                             output/Dose_module.root
/gate/actor/DoseActor/save
output/864/2e8/1/Dose_module.mhd
#/gate/actor/DoseActor/save                             output/Dose_module.txt

/gate/actor/DoseActor/stepHitType                       random
/gate/actor/DoseActor/setResolution                     864 864 1
/gate/actor/DoseActor/enableEdep                        true
/gate/actor/DoseActor/enableNumberOfHits                true
```

B. Attachments

This section refers to the separately handed in attachments, which consist of whole simulation setups and their outputs, schematics, macro files for the image analysis and more.

B.1. GATE documentation

Filename: OpenGATE_documentation_en_20210131.pdf
File path: Attachments\GATE documentation
File description: Contains the for this thesis used edition of the OpenGate documentation

B.2. LuCi schematics

B.2.1. Cabinet and granite blocks

Filename: cabinet and granite blocks.pdf
File path: Attachments\LuCi schematics
File description: Contains the drawing and measurements of the cabinet and granite blocks of LuCi

B.2.2. Detector holder

Filename: detector holder.pdf
File path: Attachments\LuCi schematics
File description: Contains the drawing and measurements of the detector holder of LuCi

B.2.3. Object holder

Filename: object holder.pdf
File path: Attachments\LuCi schematics
File description: Contains the drawing and measurements of the object holder of LuCi

B.3. Image and data analysis

B.3.1. Fiji macro-file

B.3.1.1. 1 image (2-datasets)

Filename: Macro_sg10.ijm
File path: Attachments\GATE simulations\Image_data analysis\Macro
File description: Contains the Fiji macro file used for the analysis of an individual image

B.3.1.2. 16 images (bootstrapping)

Filename: Macro_sg10_all.ijm
File path: Attachments\GATE simulations\Image_data analysis\Macro
File description: Contains the Fiji macro file used for the automatic analysis of a batch of 16 images

B.3.2. Data analysis

Filename: data_analysis.xlsx
File path: Attachments\GATE simulations\Image_data analysis
File description: Contains the results for the 2-datasets and bootstrapping method as well as the further analysis and visualization

B.4. GATE simulations and output

B.4.1. Physics processes

B.4.1.1. Physics lists

Filename: -
File path: Attachments\GATE simulations\PhysicsProcesses_PhysicsLists
File description: Contains the macro-files for the simulation as well as the histograms

B.4.1.2. Particle filters

Filename: -
File path: Attachments\GATE simulations\PhysicsProcesses_ParticleFilters
File description: Contains the macro-files for the simulation as well as the histograms

B.4.2. Production threshold

Filename: -
File path: Attachments\GATE simulations\ProductionThreshold
File description: Contains the macro-files for the simulation as well as the histograms

B.4.3. Scattered radiation – scatter grid

B.4.3.1. Configuration (p)

Filename: -
File path: Attachments\GATE simulations\Scattered radiation - scatter grid\p
File description: Contains the macro-files for the simulation as well as the output and image analysis

B.4.3.2. Configuration (p + cab)

Filename: -
File path: Attachments\GATE simulations\Scattered radiation - scatter grid\p+cab
File description: Contains the macro-files for the simulation as well as the output and image analysis

B.4.3.3. Configuration (p + gran)

Filename: -
File path: Attachments\GATE simulations\Scattered radiation - scatter grid\p+gran
File description: Contains the macro-files for the simulation as well as the output and image analysis

B.4.3.4. Configuration (p + cab + gran)

Filename: -
File path: Attachments\GATE simulations\Scattered radiation - scatter grid\p+cab+gran
File description: Contains the macro-files for the simulation as well as the output and image analysis

B.4.3.5. Configuration (p + cabs + gran)

Filename: -
File path: Attachments\GATE simulations\Scattered radiation - scatter grid\p+cabs+gran
File description: Contains the macro-files for the simulation as well as the output and image analysis

B.4.3.6. Configuration (pmx- + cab + gran)

Filename: -
File path: Attachments\GATE simulations\Scattered radiation - scatter grid\pmx-+cab+gran
File description: Contains the macro-files for the simulation as well as the output and image analysis

B.4.3.7. Configuration (pmx- + cab + gran + dh + oh)

Filename: -
File path: Attachments\GATE simulations\Scattered radiation - scatter grid\pmx-+cab+gran+dh+oh
File description: Contains the macro-files for the simulation as well as the output and image analysis

B.4.4. Collected data of simulation development

Filename: -
File path: Attachments\GATE simulations\Collected data of simulation development
File description: Contains simulations performed during the simulation development